

The joint projected and skew normal; a distribution for poly-cylindrical data

Gianluca Mastrantonio

Department of Mathematics, Polytechnic of Turin, Turin, Italy

Abstract

The contribution of this work is the introduction of a multivariate circular-linear (or poly-cylindrical) distribution obtained by combining the projected and the skew normal. We show the flexibility of our proposal, its property of closure under marginalization and how to quantify multivariate dependence.

Due to a non-identifiability issue that our proposal inherits from the projected normal, a computational problem arises. We overcome it in a Bayesian framework, adding suitable latent variables and showing that posterior samples can be obtained with a post-processing of the estimation algorithm output. Under specific prior choices, this approach enables us to implement a Markov chain Monte Carlo algorithm relying only on Gibbs steps, where the updates of the parameters are done as if we were working with a multivariate normal likelihood. The proposed approach can be also used with the projected normal.

As a proof of concept, on simulated examples we show the ability of our algorithm in recovering the parameters values and to solve the identification problem. Then the proposal is used in a real data example, where the turning-angles (circular variables) and the logarithm of the step-lengths (linear variables) of four zebras are jointly modelled.

Keywords: Multivariate Distribution, Circular Data, Circular-linear Distribution, Projected Normal, Skew Normal

1. Introduction

The analysis of circular data, i.e., observations with support the unit circle, requires specific statistical tools since the circular domain is intrinsically different from the real line, that is the domain of linear variables, and this inhibits the use of standard statistics that if not properly modified lead to not interpretable results; for a general review see [16], [22] or [34]. A similar type of problem holds for circular densities that, besides being non negative and to integrate to 1, should possess the property of “invariance” [27], i.e., they must be a location model under the group of rotations and reflections of the circle. This property, that expresses the need of densities that can represent equivalently the same phenomena under different reference systems, is peculiar of circular densities and it is sometimes overlooked [27].

Circular data are often observed along with linear ones and they are called cylindrical if bivariate, otherwise poly-cylindrical. For example in marine research wind and wave directions are modelled with wind speed and wave height [8, 25, 39] and, in ecology, animal behaviour is described using measures of speed and direction, e.g., step-length and turning-angle [9, 19, 31, 33]. In most of the applications cylindrical data are modelled assuming independence between the circular and linear components, see for example [8], [20] or [30]. Ignoring dependence can lead to misleading inference since we are not considering a component of the data that can help in understanding the phenomenon under study [see for example 28]. In the literature, to date, no poly-cylindrical distributions have been proposed and there are only few distributions for cylindrical data; the best known examples are the ones of [2], [17], [23] and the new density of [1]. The aim of this work is to introduce what is, to the best of our knowledge, the first poly-cylindrical distribution.

Circular and linear variables live in very different spaces and the definition of a mixed-domain distribution is not easy. The issue is even more complicated if we require flexibility, interpretable parameters and the possibility to define an efficient and easy to implement estimation algorithm. We decide to put ourselves in a Bayesian framework because, as we show in Section 3.1, using standard Markov chain Monte Carlo (MCMC) methods we are able to propose an algorithm with the required characteristics while Monte Carlo (MC) procedures [7, 36] allow us to obtain posterior distributions for all the statistics we may need to describe the results.

Since circular observations show often bimodality, see for example [38] or [40], our aim is to propose a distribution with circular marginals that can model such data. In the literature the most known bimodal circular distributions are the projected normal (\mathcal{PN}) [40] and the generalized von Mises [10]. The former can be easily generalized to the multivariate setting and it has an interesting augmented density representation, based on a normal probability density function (pdf), that can be used to define circular-linear dependence. The \mathcal{PN} is very flexible [see for example 26, 41] with shapes that range from unimodal and symmetric to bimodal and antipodal, it is closed under marginalization and, as we show in the Appendix, it has the invariance property. On the other hand, multivariate extensions of the generalized von Mises are not easy to handle and, in our opinion, it not straightforward to use it as a component of a poly-cylindrical distribution.

We define our proposal constructively, starting from the \mathcal{PN} and choosing a distribution for the linear component that, taking advantage of the \mathcal{PN} augmented density representation, allows us to define a poly-cylindrical distribution whose parameters can be easily estimated with MCMC algorithms and it is flexible enough to model real data.

For the linear component we use a skew normal, that is a generalization of the Gaussian distribution which allows more flexibility introducing asymmetry in the normal density. Its first univariate version was proposed by [4] and following works introduced multivariate extensions and different formalizations; see for example [5], [13], [18] or [37]. Among these, we found the one of [37] (hereafter \mathcal{SSN}) interesting: it can be closed under marginalization and it has an augmented density representation that, as the \mathcal{PN} , is based on a normal pdf.

Using this particular form of the skew normal distribution, due to the properties listed above, we are able to define the *joint projected and skew normal* (\mathcal{JPSN}) poly-cylindrical distribution by introducing dependence in the normal pdfs of the augmented representations. The distribution retains the \mathcal{PN} and \mathcal{SSN} as marginal distributions and is closed under marginalization, i.e., any subset of circular and linear variables is \mathcal{JPSN} distributed. The MCMC algorithm we propose can be based only on Gibbs steps, updating parameters as if we were working with a multivariate normal likelihood. The density cannot be expressed in closed form but, from the point of view of model fitting, since we are able to estimate its parameters easily we do not consider this an issue.

The \mathcal{JPSN} has the same identification problem of the \mathcal{PN} [40], but we show that posterior values can be obtained by a post-processing of the MCMC algorithm based on the non-identifiable likelihood. The proposed algorithm can be also used with the univariate and multivariate \mathcal{PN} and the spherical \mathcal{PN} distribution of [14], solving their identification problem in a new way.

The algorithm, tested on simulated datasets, shows its ability in retrieving the parameters used to simulate the data and posterior samples do not suffer from an identification issue. We used the \mathcal{JPSN} to jointly model the logarithm of step-lengths and turning-angles of 4 zebras observed in Botswana (Africa). A comparison based on the continuous rank probability scores (CRPSs) [11, 12] between our proposal, the cylindrical distribution of [1] and a cylindrical version of the \mathcal{JPSN} , i.e., assuming independence between zebras, is provided, showing that ignoring multivariate dependence can lead to loss of predictive ability.

The paper is organized as follows. Section 2 is devoted to the constructive definition of the distribution. In Section 3 we introduce the identification problem and how to estimate the \mathcal{JPSN} parameters. The proposal is applied to simulated examples in Section 4.1 and the real data application is shown in Section 4.2. The paper ends with concluding remarks in Section 5. In the Appendix we prove the invariance property of the \mathcal{PN} and we show MCMC implementation details.

2. The joint projected and skew normal distribution

In this section we build the poly-cylindrical density by first introducing the circular and linear marginals and then showing how to induce dependence.

2.1. The projected normal distribution

The \mathcal{PN} is a distribution for a p -dimensional vector $\Theta = \{\Theta_i\}_{i=1}^p$ of circular variables, i.e., $\Theta_i \in [0, 2\pi)$ is an angle expressed in radian, obtained starting from a $2p$ -dimensional vector $\mathbf{W} = \{\mathbf{W}_i\}_{i=1}^p$, where $\mathbf{W}_i = (W_{i1}, W_{i2})^\top \in \mathbb{R}^2$, distributed as a $2p$ -variate normal with mean vector $\boldsymbol{\mu}_w$ and covariance matrix $\boldsymbol{\Sigma}_w$. \mathbf{W}_i , normally distributed with parameters $\{\boldsymbol{\mu}_{w_i}, \boldsymbol{\Sigma}_{w_i}\}$, is a point in the 2-dimensional space expressed using the Cartesian system. The same point can

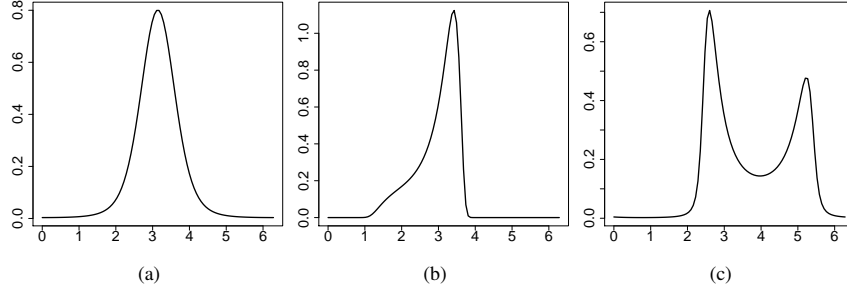


Figure 1: Univariate projected normal densities under three sets of parameters: (a) $\boldsymbol{\mu}_{w_i} = \begin{pmatrix} 2 \\ 0 \end{pmatrix}$, $\boldsymbol{\Sigma}_{w_i} = \begin{pmatrix} 1 & 0 \\ 0 & 1 \end{pmatrix}$; (b) $\boldsymbol{\mu}_{w_i} = \begin{pmatrix} 2 \\ 0 \end{pmatrix}$, $\boldsymbol{\Sigma}_{w_i} = \begin{pmatrix} 1 & 0.9 \\ 0.9 & 1 \end{pmatrix}$; (c) $\boldsymbol{\mu}_{w_i} = \begin{pmatrix} -0.1 \\ -0.2 \end{pmatrix}$, $\boldsymbol{\Sigma}_{w_i} = \begin{pmatrix} 1 & -0.9 \\ -0.9 & 1 \end{pmatrix}$

be also represented in polar coordinates with the angle Θ_i and the distance vector $R_i \in \mathbb{R}^+$. Between \mathbf{W}_i , Θ_i and R_i the following relations exist:

$$\Theta_i = \text{atan}^* \left(\frac{W_{i2}}{W_{i1}} \right) \quad (1)$$

and

$$\mathbf{W}_i = R_i \begin{pmatrix} \cos \Theta_i \\ \sin \Theta_i \end{pmatrix}, \quad R_i = \|\mathbf{W}_i\|,$$

where

$$\text{atan}^* \left(\frac{S}{C} \right) = \begin{cases} \text{atan} \left(\frac{S}{C} \right) & \text{if } C > 0, S \geq 0, \\ \frac{\pi}{2} & \text{if } C = 0, S > 0, \\ \text{atan} \left(\frac{S}{C} \right) + \pi & \text{if } C < 0, \\ \text{atan} \left(\frac{S}{C} \right) + 2\pi & \text{if } C \geq 0, S < 0, \\ \text{undefined} & \text{if } C = 0, S = 0, \end{cases}$$

is a modified arctangent function used to define a quadrant-specific inverse of the tangent.

If we transform each \mathbf{W}_i in $(\Theta_i, R_i)^\top$ the Jacobian of the transformation is $\prod_{i=1}^p R_i$ and then the joint density of $(\boldsymbol{\Theta}, \mathbf{R})^\top$, where $\mathbf{R} = \{R_i\}_{i=1}^p$, is given by

$$f(\boldsymbol{\theta}, \mathbf{r}) = \prod_{i=1}^p r_i \phi_{2p}(\mathbf{w} | \boldsymbol{\mu}_w, \boldsymbol{\Sigma}_w), \quad (2)$$

where $f(\cdot)$ indicates the density of its arguments, \mathbf{r} is a realization of \mathbf{R} , $\phi_{2p}(\mathbf{w} | \boldsymbol{\mu}_w, \boldsymbol{\Sigma}_w)$ is the pdf evaluated at \mathbf{w} of a $2p$ -variate normal distribution with mean $\boldsymbol{\mu}_w$ and covariance matrix $\boldsymbol{\Sigma}_w$; here \mathbf{w} must be seen as a function of $(\boldsymbol{\theta}, \mathbf{r})^\top$.

The marginal density of $\boldsymbol{\Theta}$, obtained by integrating out \mathbf{R} in (2), is a p -variate projected normal with parameters $\boldsymbol{\mu}_w$ and $\boldsymbol{\Sigma}_w$, i.e., $\boldsymbol{\Theta} \sim \mathcal{PN}_p(\boldsymbol{\mu}_w, \boldsymbol{\Sigma}_w)$. As shown in [40], the \mathcal{PN} can be symmetric, asymmetric and bimodal; univariate shapes are depicted in Figure 1.

A closed form expression for the \mathcal{PN}_p density is only available in the univariate case ($p = 1$) and it is

$$f(\theta_i) = \frac{\phi_2(\boldsymbol{\mu}_{w_i} | \mathbf{0}_2, \boldsymbol{\Sigma}_{w_i}) + |\boldsymbol{\Sigma}_{w_i}|^{-1} D(\theta_i) \Phi_1(D(\theta_i) | 0, 1) \phi_1 \left(|\boldsymbol{\Sigma}_{w_i}|^{-1} C(\theta_i)^{-1/2} (\mu_{w_{i1}} \sin \theta_i - \mu_{w_{i2}} \cos \theta_i) \right)}{C(\theta_i)},$$

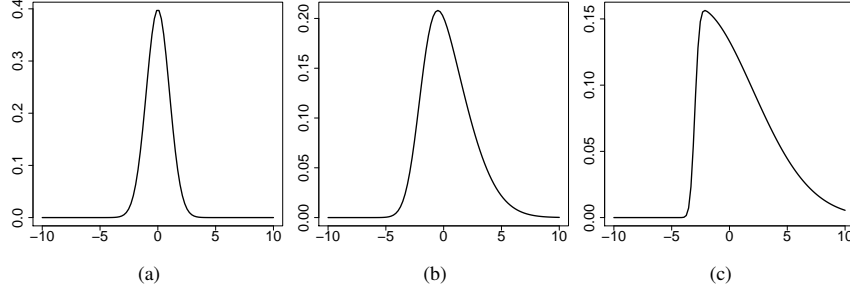


Figure 2: Univariate skew normal densities under three sets of parameters: (a) $\mu_y = 0$, $\Sigma_y = 1$, $\lambda = 0$; (b) $\mu_y = -2$, $\Sigma_y = 1$, $\lambda = 3$; (c) $\mu_y = -3$, $\Sigma_y = 0.1$, $\lambda = 5$.

where

$$C(\theta_i) = |\Sigma_{w_i}|^{-2} (\sigma_{w_{i2}}^2 \cos^2 \theta_i - \rho_{w_i} \sigma_{w_{i1}} \sigma_{w_{i2}} \sin 2\theta_i + \sigma_{w_{i1}}^2 \sin^2 \theta_i),$$

$$D(\theta_i) = \frac{|\Sigma_{w_i}|^{-2} (\mu_{w_{i1}} \sigma_{w_{i2}} (\sigma_{w_{i2}} \cos \theta_i - \rho_{w_i} \sigma_{w_{i1}} \sin \theta_i) + \mu_{w_{i2}} \sigma_{w_{i1}} (\sigma_{w_{i1}} \sin \theta_i - \rho_{w_i} \sigma_{w_{i2}} \cos \theta_i))}{\sqrt{C(\theta_i)}},$$

$\Phi_\ell(\cdot, \cdot)$ indicates the normal ℓ -variate cumulative distribution function with given mean vector and covariance matrix, $\mathbf{0}_\ell$ is a vector of 0s of length ℓ , $\mu_{w_{ij}}$ and $\sigma_{w_{ij}}^2$ are the mean and variance of W_{ij} and ρ_{w_i} is the correlation between W_{i1} and W_{i2} .

In practical applications [see for example 24, 26, 41] it is generally preferable to work with the pair $(\Theta, \mathbf{R})^\top$ that has the nice closed form density given in equation (2), treating \mathbf{R} as a vector of latent variables.

The multivariate \mathcal{PN} is closed under marginalization since $\Theta_A \sim \mathcal{PN}_{n_a}(\mu_{w,A}, \Sigma_{w,A})$, where $A \subset \{1, \dots, p\}$, n_a indicates the cardinality of the set A and $\{\mu_{w,A}, \Sigma_{w,A}\}$ are mean and covariance matrix of \mathbf{W}_A . Moreover, as we show in Appendix A, the univariate \mathcal{PN} possesses the invariance property and then inference does not depend on the reference system chosen for the circular variables [27].

2.2. The skew normal distribution

We now introduce the skew normal distribution of [37] as the distribution of a q -dimensional vector $\mathbf{Y} = \{Y_j\}_{j=1}^q$, with $Y_j \in \mathbb{R}$. Let μ_y be a vector of length q , Σ_y be a $q \times q$ non-negative definite (nnd) matrix and $\Lambda = \text{diag}(\lambda)$ be a $q \times q$ diagonal matrix with diagonal elements $\lambda = \{\lambda_i\}_{i=1}^q \in \mathbb{R}^q$. We say that \mathbf{Y} is distributed accordingly to a q -variate skew normal with parameters μ_y, Σ_y and λ ($\mathbf{Y} \sim \mathcal{SSN}_q(\mu_y, \Sigma_y, \lambda)$) if it has pdf

$$f(\mathbf{y}) = 2^q \phi_q(\mathbf{y} | \mu_y, \Upsilon) \Phi_q(\Lambda^\top \Upsilon^{-1}(\mathbf{y} - \mu_y) | \mathbf{0}_q, \Gamma), \quad (3)$$

where $\Upsilon = \Sigma_y + \Lambda \Lambda^\top$, $\Gamma = \mathbf{I}_q - \Lambda^\top \Upsilon^{-1} \Lambda$ and \mathbf{I}_q is the identity matrix of dimension q . Although in [37] Λ is defined as a full matrix, here we constrain it to be diagonal to have a \mathcal{SSN} closed under marginalization; the same property will be inherited by our poly-cylindrical distribution (see Section 2.3). From (3) we clearly see that $\mathbf{Y} \sim \mathcal{N}_q(\mu_y, \Sigma_y)$ if Λ is a null matrix and for this reason it is called the *skew parameter*. Examples of univariate \mathcal{SSN} densities are shown in Figure 2.

The \mathcal{SSN} has a nice stochastic representation [3] that is useful for the definition of the poly-cylindrical distribution. Let $\mathbf{D} \sim \mathcal{HN}_q(\mathbf{0}_q, \mathbf{I}_q)$, where $\mathcal{HN}_q(\cdot, \cdot)$ indicates the q -dimensional half normal [32], and $\mathbf{H} \sim \mathcal{N}_q(\mathbf{0}_q, \Sigma_y)$, then \mathbf{Y} can be written as

$$\mathbf{Y} = \mu_y + \Lambda \mathbf{D} + \mathbf{H}. \quad (4)$$

From (4) we can see that $\mathbf{Y} | \mathbf{D} = \mathbf{d}$ is normally distributed with mean $\mu_y + \Lambda \mathbf{d}$ and covariance matrix Σ_y . Consequently, the joint density of $(\mathbf{Y}, \mathbf{D})^\top$ expressed as the product of the ones of $\mathbf{Y} | \mathbf{D}$ and \mathbf{D} , is given by

$$f(\mathbf{y}, \mathbf{d}) = 2^q \phi_q(\mathbf{y} | \mu_y + \Lambda \mathbf{d}, \Sigma_y) \phi_q(\mathbf{d} | \mathbf{0}_q, \mathbf{I}_q). \quad (5)$$

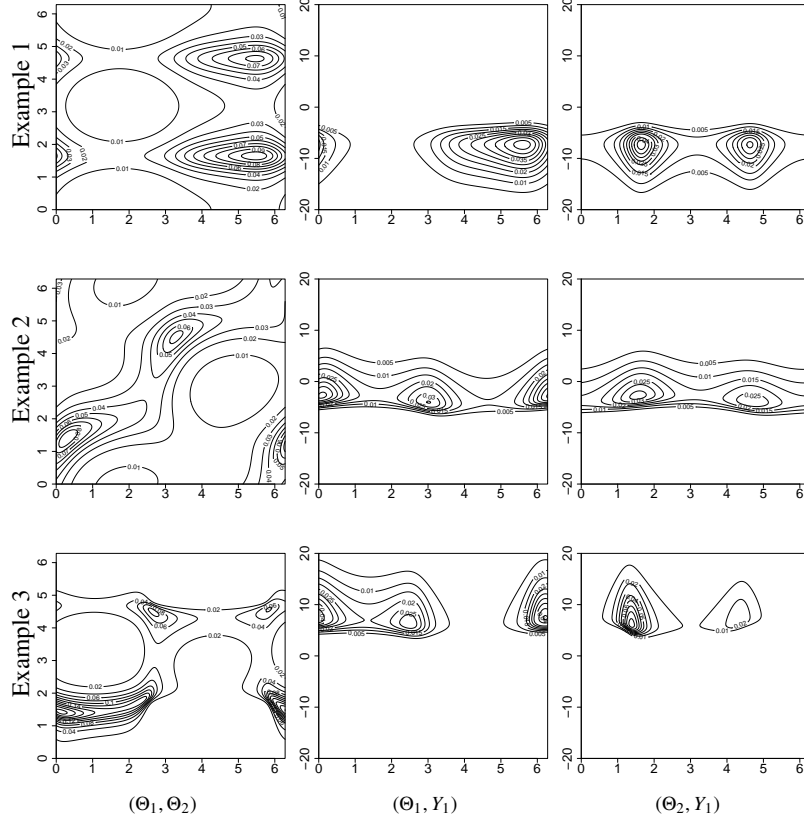


Figure 3: Bivariate marginal distributions of a $\mathcal{JPSN}_{2,1}(\mu, \Sigma, \lambda)$ under three sets of parameters (row) reported in Section 4.1. In the first column there are the marginal distributions of (Θ_1, Θ_2) , in the second those of (Θ_1, Y_1) and in the third the marginals of (Θ_2, Y_1) .

2.3. The joint linear-circular distribution

In this section we define the poly-cylindrical distribution starting from the augmented circular and linear marginals shown in equations (2) and (5). As in the previous sections, we indicate with p and q the dimensions of the vectors of circular and linear variables, respectively.

It is natural to introduce dependence between Θ and \mathbf{Y} by substituting the two normal pdfs of the augmented representation, i.e., $\phi_{2p}(\mathbf{w}|\mu_w, \Sigma_w)$ and $\phi_q(\mathbf{y}|\mu_y + \text{diag}(\lambda)\mathbf{d}, \Sigma_y)$, with a $2p + q$ normal pdf that has the two pdfs as marginals; after marginalization we obtain the density of $(\Theta, \mathbf{Y})^\top$. More precisely, we define the joint density of $(\Theta, \mathbf{R}, \mathbf{Y}, \mathbf{D})^\top$ as

$$f(\theta, \mathbf{r}, \mathbf{y}, \mathbf{d}) = 2^q \phi_{2p+q}((\mathbf{w}, \mathbf{y})^\top | \mu + (\mathbf{0}_{2p}, \text{diag}(\lambda)\mathbf{d})^\top, \Sigma) \phi_q(\mathbf{d} | \mathbf{0}_q, \mathbf{I}_q) \prod_{i=1}^p r_i, \quad (6)$$

with $\mu = (\mu_w, \mu_y)^\top$ and

$$\Sigma = \begin{pmatrix} \Sigma_w & \Sigma_{wy} \\ \Sigma_{wy}^\top & \Sigma_y \end{pmatrix}.$$

We then say that $(\Theta, \mathbf{Y})^\top$ is marginally distributed as a (p, q) -variate *joint projected and skew normal* with parameters μ, Σ and λ , i.e., $(\Theta, \mathbf{Y})^\top \sim \mathcal{JPSN}_{p,q}(\mu, \Sigma, \lambda)$. Since $(\mathbf{W}, \mathbf{Y})^\top | \mathbf{d} \sim N_{2p+q}(\mu + (\mathbf{0}_{2p}, \text{diag}(\lambda)\mathbf{d})^\top, \Sigma)$, transformation of \mathbf{W} into Θ using (1) implies that $(\Theta, \mathbf{Y})^\top$ is \mathcal{JPSN} distributed; this last remark can be used to easily simulate random samples from the \mathcal{JPSN} .

Closure under marginalization of the \mathcal{PN} and the \mathcal{SSN} shows that any subset of $(\Theta, \mathbf{Y})^\top$ is still \mathcal{JPSSN} distributed (see equation (6)) and, as limit cases, $\Theta \sim \mathcal{PN}_p(\mu_w, \Sigma_w)$ and $\mathbf{Y} \sim \mathcal{SSN}_q(\mu_y, \Sigma_y, \text{diag}(\lambda))$. The flexibility of the \mathcal{PN} and \mathcal{SSN} are then inherited by the marginal distributions of our proposal that allows also multivariate dependence between its components. Conditional densities are not standard, but from $(\mathbf{W}, \mathbf{Y})^\top | \mathbf{d} \sim N_{2p+q}(\mu + (\mathbf{0}_{2p}, \text{diag}(\lambda)\mathbf{d})^\top, \Sigma)$ we can easily see that

$$\Theta | \mathbf{y}, \mathbf{d} \sim \mathcal{PN}_p(\mu_w + \Sigma_{wy}\Sigma_y^{-1}(\mathbf{y} - \mu_y - \text{diag}(\lambda)\mathbf{d}), \Sigma_w + \Sigma_{wy}\Sigma_y^{-1}\Sigma_{wy}^\top)$$

and

$$\mathbf{Y} | \theta, \mathbf{r} \sim \mathcal{SSN}_q(\mu_y + \text{diag}(\lambda)\mathbf{d} + \Sigma_{wy}\Sigma_w^{-1}(\mathbf{w} - \mu_w), \Sigma_y + \Sigma_{wy}\Sigma_w^{-1}\Sigma_{wy}^\top).$$

\mathcal{JPSSN} shapes are depicted in Figure 3.

Notice that $\Theta_i \perp \Theta_j$, where \perp indicates independence, iff $\mathbf{W}_i \perp \mathbf{W}_j$ and, by construction, matrix Σ_{wy} rules the circular-linear dependence since iff $\mathbf{W}_i \perp Y_j$ then $\Theta_i \perp Y_j$. Parameters μ_y and Σ_y are easily interpretable since $E(\mathbf{Y}) = \mu_y + \lambda\sqrt{2/\pi}$, $\text{Var}(\mathbf{Y}) = \Sigma_y + (1 - 2/\pi)\text{diag}(\lambda)\text{diag}(\lambda)$ and if $[\Sigma_y]_{j,k} = 0$, where $[\Sigma_y]_{j,k}$ indicates the element positioned in the j^{th} row and k^{th} column, then Y_j and Y_k are independent. λ controls the skewness of the linear component and Y_i is normally distributed if $\lambda_i = 0$. Parameters μ_{w_i} and Σ_{w_i} determine the shape of the density of Θ_i , that is always \mathcal{PN} . It is not clear how changing one of the element of μ_{w_i} or Σ_{w_i} affects the density, but special cases exist: a circular uniform distribution is obtained with $\mu_{w_i} = \mathbf{0}_2$ and $\Sigma_{w_i} = d\mathbf{I}_2$, $\mu_{w_i} = \mathbf{0}_2$ produces an antipodal density and $\mathcal{PN}(\mu_{w_i}, d\mathbf{I}_2)$ is unimodal and symmetric. All the other statistics of the distribution that cannot be computed directly from the parameters, e.g., the circular mean, can be approximated with MC procedures.

3. Identifiability and Bayesian inference

Let \mathbf{C}_w be a $2p \times 2p$ diagonal matrix with $(2(i-1) + j) - \text{th}$ entry equal to $c_i > 0$, where $i = 1, \dots, p$ and $j = 1, 2$. Then, since

$$\Theta_i = \text{atan}^* \frac{W_{i2}}{W_{i1}} = \text{atan}^* \frac{c_i W_{i2}}{c_i W_{i1}}, \quad (7)$$

the two random vectors $\mathbf{W}_i \sim \mathcal{N}_2(\mu_w, \Sigma_w)$ and $\mathbf{C}_w \mathbf{W}_i \sim \mathcal{N}_{2p}(\mathbf{C}_w \mu_w, \mathbf{C}_w \Sigma_w \mathbf{C}_w)$ produce the same Θ , i.e., the c_i s cancel out in equation (7). It follows that $\{\mu_w, \Sigma_w\}$ and $\{\mathbf{C}_w \mu_w, \mathbf{C}_w \Sigma_w \mathbf{C}_w\}$ represent the same \mathcal{PN} density which is then not identifiable.

The \mathcal{JPSSN} is based on the \mathcal{PN} , that is also its circular marginal distribution, and it has the same identification issue; for identifiability constraints on the parameters space are needed. Following and extending [40], we set to one the variance of each W_{i2} and from now on, to avoid confusion, we indicate $\{\mu, \Sigma, \mathbf{W}, \mathbf{R}\}$ as $\{\tilde{\mu}, \tilde{\Sigma}, \tilde{\mathbf{W}}, \tilde{\mathbf{R}}\}$ when such constraints are imposed; $\lambda, \mathbf{D}, \mu_y$ and Σ_y are always identified since they are related only to the linear component. Let

$$\mathbf{C} = \begin{pmatrix} \mathbf{C}_w & \mathbf{0}_{2p,q} \\ \mathbf{0}_{2p,q}^\top & \mathbf{I}_q \end{pmatrix},$$

where $\mathbf{0}_{2p,q}^\top$ is a $2p \times q$ zero matrix, then the sets $\{\tilde{\mu}, \tilde{\Sigma}, \lambda\}$ and $\{\mu, \Sigma, \lambda\}$ with

$$\begin{aligned} \mu &= \mathbf{C}\tilde{\mu}, \\ \Sigma &= \mathbf{C}\tilde{\Sigma}\mathbf{C}, \end{aligned}$$

produce the same \mathcal{JPSSN} density and the following relation holds:

$$\begin{aligned} f(\theta, \tilde{\mathbf{r}}, \mathbf{y}, \mathbf{d}) &= 2^q \phi_{2p+q}((\tilde{\mathbf{w}}, \mathbf{y})^\top | \tilde{\mu} + (\mathbf{0}_{2p}, \text{diag}(\lambda)\mathbf{d})^\top, \tilde{\Sigma}) \phi_q(\mathbf{d} | \mathbf{0}_q, \mathbf{I}_q) \prod_{i=1}^p \tilde{r}_i = \\ &= 2^q \phi_{2p+q}(\mathbf{C}(\tilde{\mathbf{w}}, \mathbf{y})^\top | \mathbf{C}\tilde{\mu} + (\mathbf{0}_{2p}, \text{diag}(\lambda)\mathbf{d})^\top, \mathbf{C}\tilde{\Sigma}\mathbf{C}) \phi_q(\mathbf{d} | \mathbf{0}_q, \mathbf{I}_q) \prod_{i=1}^p c_i \tilde{r}_i. \end{aligned} \quad (8)$$

Notice that there is a one-to-one relation between sets $\{\mu, \Sigma\}$ and $\{\tilde{\mu}, \tilde{\Sigma}, \mathbf{C}\}$ since $c_i = \sqrt{[\Sigma]_{2i,2i}}$.

Due to the unavailability of MCMC algorithms for a constrained covariance matrix estimate, a computational problem arises and we show how to overcome it in the next section.

3.1. The MCMC algorithm

Suppose to have T observations drawn from a (p, q) -variate \mathcal{JPSN} , i.e., $(\mathbf{\Theta}_t, \mathbf{Y}_t)^\top \sim \mathcal{JPSN}_{p,q}(\tilde{\boldsymbol{\mu}}, \tilde{\boldsymbol{\Sigma}}, \lambda)$ with $t = 1, \dots, T$. As the \mathcal{JPSN} does not have a closed form density, we introduce $\tilde{\mathbf{R}}_t = \{\tilde{R}_{ti}\}_{i=1}^p$ and \mathbf{D}_t as latent variables and letting $g_1(\tilde{\boldsymbol{\mu}}, \tilde{\boldsymbol{\Sigma}}|\lambda)g_2(\lambda)$ be the prior distribution, we want to evaluate the posterior of $\{\{\tilde{\mathbf{R}}_t\}_{t=1}^T, \{\mathbf{D}_t\}_{t=1}^T, \tilde{\boldsymbol{\mu}}, \tilde{\boldsymbol{\Sigma}}, \lambda\}$ given by

$$\frac{\prod_{t=1}^T 2^q \phi_{2p+q}((\tilde{\mathbf{w}}_t, \mathbf{y}_t)^\top | \tilde{\boldsymbol{\mu}} + (\mathbf{0}_{2p}, \text{diag}(\lambda)\mathbf{d}_t)^\top, \tilde{\boldsymbol{\Sigma}}) \phi_q(\mathbf{d}_t | \mathbf{0}_q, \mathbf{I}_q) \prod_{i=1}^p \tilde{r}_{ti} g_1(\tilde{\boldsymbol{\mu}}, \tilde{\boldsymbol{\Sigma}}|\lambda) g_2(\lambda)}{Z(\{\boldsymbol{\theta}_t, \mathbf{y}_t\}_{t=1}^T)}, \quad (9)$$

where $Z(\{\boldsymbol{\theta}_t, \mathbf{y}_t\}_{t=1}^T)$ is the normalization constant. Some difficulties arise in the definition of $g_1(\cdot)$ since its domain must contain the space of constrained nnd matrices and, to the best of our knowledge, no priors with such domain are available.

Our proposed MCMC algorithm starts defining a prior $f(\boldsymbol{\mu}, \boldsymbol{\Sigma}|\lambda)$ over $\{\boldsymbol{\mu}, \boldsymbol{\Sigma}\}$. We indicate with $f^*(\mathbf{C}, \tilde{\boldsymbol{\mu}}, \tilde{\boldsymbol{\Sigma}}|\lambda)$ the distribution over $\{\mathbf{C}, \tilde{\boldsymbol{\mu}}, \tilde{\boldsymbol{\Sigma}}\}$ induced by $f(\boldsymbol{\mu}, \boldsymbol{\Sigma}|\lambda)$ and we define $g_1(\tilde{\boldsymbol{\mu}}, \tilde{\boldsymbol{\Sigma}}|\lambda)$ as

$$g_1(\tilde{\boldsymbol{\mu}}, \tilde{\boldsymbol{\Sigma}}|\lambda) = \int_{\mathbb{R}^+} \dots \int_{\mathbb{R}^+} f^*(\mathbf{C}, \tilde{\boldsymbol{\mu}}, \tilde{\boldsymbol{\Sigma}}|\lambda) dc_1 \dots dc_p. \quad (10)$$

Then, using (8) and (10) we can write (9) as

$$\begin{aligned} \int_{\mathbb{R}^+} \dots \int_{\mathbb{R}^+} \prod_{t=1}^T 2^q \phi_{2p+q}(\mathbf{C}(\tilde{\mathbf{w}}_t, \mathbf{y}_t)^\top | \mathbf{C}\tilde{\boldsymbol{\mu}} + (\mathbf{0}_{2p}, \text{diag}(\lambda)\mathbf{d}_t)^\top, \mathbf{C}\tilde{\boldsymbol{\Sigma}}\mathbf{C}) \times \\ \frac{\phi_q(\mathbf{d}_t | \mathbf{0}_q, \mathbf{I}_q) \prod_{i=1}^p c_i \tilde{r}_{ti} f^*(\mathbf{C}, \tilde{\boldsymbol{\mu}}, \tilde{\boldsymbol{\Sigma}}|\lambda) g_2(\lambda)}{Z(\{\boldsymbol{\theta}_t, \mathbf{y}_t\}_{t=1}^T)} dc_1 \dots dc_p, \end{aligned} \quad (11)$$

and if we transform $\{\mathbf{C}, \{\tilde{\mathbf{R}}_t\}_{t=1}^T, \tilde{\boldsymbol{\mu}}, \tilde{\boldsymbol{\Sigma}}\}$ into $\{\{\mathbf{R}_t\}_{t=1}^T, \boldsymbol{\mu}, \boldsymbol{\Sigma}\}$, the integrand of equation (11) becomes

$$\frac{\prod_{t=1}^T \phi_{2p+q}((\mathbf{w}_t, \mathbf{y}_t)^\top | \boldsymbol{\mu} + (\mathbf{0}_{2p}, \text{diag}(\lambda)\mathbf{d}_t)^\top, \boldsymbol{\Sigma}) \phi_q(\mathbf{d}_t | \mathbf{0}_q, \mathbf{I}_q) \prod_{i=1}^p r_{ti} f(\boldsymbol{\mu}, \boldsymbol{\Sigma}|\lambda) g_2(\lambda)}{Z(\{\boldsymbol{\theta}_t, \mathbf{y}_t\}_{t=1}^T)}. \quad (12)$$

Then, relying on standard MC integration rules [see for example 7, 36], a set of B draws from (9) is obtained by taking B samples of $\{\{\mathbf{R}_t\}_{t=1}^T, \{\mathbf{D}_t\}_{t=1}^T, \boldsymbol{\mu}, \boldsymbol{\Sigma}, \lambda\}$ from (12) and transforming them to $\{\{\tilde{\mathbf{R}}_t\}_{t=1}^T, \{\mathbf{D}_t\}_{t=1}^T, \tilde{\boldsymbol{\mu}}, \tilde{\boldsymbol{\Sigma}}, \lambda\}$.

In a schematic way our proposal is

- to define a prior over $\{\boldsymbol{\mu}, \boldsymbol{\Sigma}, \lambda\}$ that induces a prior $g_1(\cdot)$ (see equation (10));
- to obtain a set of samples of $\{\{\mathbf{R}_t\}_{t=1}^T, \{\mathbf{D}_t\}_{t=1}^T, \boldsymbol{\mu}, \boldsymbol{\Sigma}, \lambda\}$ from distribution (12);
- to transform the posterior samples of $\{\{\mathbf{R}_t\}_{t=1}^T, \boldsymbol{\mu}, \boldsymbol{\Sigma}\}$ into $\{\{\tilde{\mathbf{R}}_t\}_{t=1}^T, \tilde{\boldsymbol{\mu}}, \tilde{\boldsymbol{\Sigma}}\}$ after the model fitting.

The resulting posterior samples are from the distribution of interest (equation (9)). The proposed MCMC algorithm can be used with the \mathcal{JPSN} , the univariate projected normal ($q = 0$ and $p = 1$), the multivariate projected normal ($q = 0$) and also with the proposal of [14], i.e., a distribution defined over the K -dimensional sphere, since all of them share the same identification problem.

There are no restrictions on the choice of $g_1(\cdot)$ and $g_2(\cdot)$ but, as shown in Appendix B, if ease of implementation and conjugate priors are required, a normal inverse-Wishart (\mathcal{NIW}) can be used for $\{\boldsymbol{\mu}, \boldsymbol{\Sigma}\}$ and a normal for λ ; these are the ones we use in the examples of Section 4. Regardless of the priors chosen, the updates of \mathbf{D}_t and R_{ti} can be done using Gibbs steps.

4. Examples

4.1. Synthetic data

The aim of these simulated examples is to prove that the proposed MCMC algorithm is able to retrieve the parameters used to simulate the data and to solve the identification problem. We simulate 3 datasets with $p = 2$, $q = 1$, i.e.,

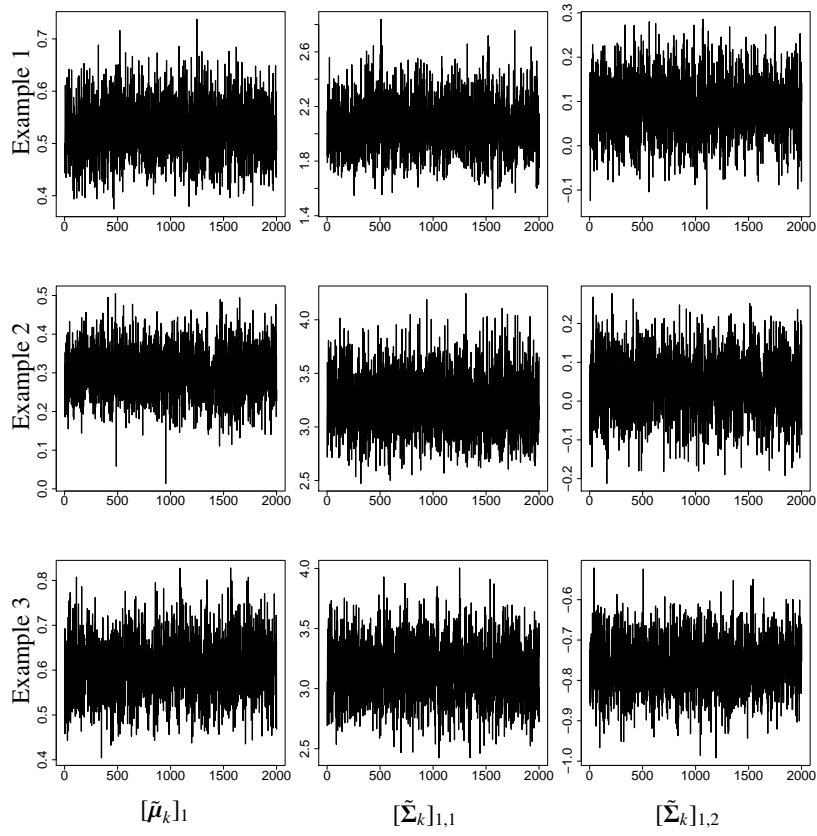


Figure 4: Simulated examples - trace plots of parameters $[\tilde{\mu}_k]_1$, $[\tilde{\Sigma}_k]_{1,1}$ and $[\tilde{\Sigma}_k]_{1,2}$ (columns) in the three examples (rows)

	Example		
	k=1	k=2	k=3
$[\hat{\tilde{\mu}}_k]_1$	0.529	0.301	0.608
CI	(0.428 0.638)	(0.179 0.427)	(0.480 0.738)
$[\hat{\tilde{\mu}}_k]_2$	-0.943	0.207	0.5
CI	(-1.029 -0.858)	(0.137 0.280)	(0.428 0.576)
$[\hat{\tilde{\mu}}_k]_3$	-0.112	-0.02	0.007
CI	(-0.145 -0.080)	(-0.068 0.029)	(-0.023 0.036)
$[\hat{\tilde{\mu}}_k]_4$	0.095	0.111	0.503
CI	(0.020 0.163)	(0.041 0.178)	(0.429 0.576)
$[\hat{\tilde{\mu}}_k]_5$	-5.095	-4.765	4.705
CI	(-5.415 -4.780)	(-4.925 -4.596)	(4.489 5.105)
$\hat{\lambda}_k$	-4.941	4.872	6.237
CI	(-5.320 -4.561)	(4.630 5.135)	(5.920 6.556)

Table 1: Simulated examples - posterior mean estimates ($\hat{\cdot}$) and 95% credible intervals (CI) of $\tilde{\mu}_k$ and λ_k .

two circular variables and 1 linear, $T = 1000$ and parameters

$$\tilde{\mu}_1 = \begin{bmatrix} 0.5 \\ -1.0 \\ -0.1 \\ 0.1 \\ -5.0 \end{bmatrix}, \quad \tilde{\mu}_2 = \begin{bmatrix} 0.2 \\ 0.2 \\ 0.0 \\ 0.1 \\ -5.0 \end{bmatrix}, \quad \tilde{\mu}_3 = \begin{bmatrix} 0.5 \\ 0.5 \\ 0.0 \\ 0.5 \\ 5.0 \end{bmatrix},$$

	j=1	j=2	j=3	j=4	j=5
$[\hat{\Sigma}_1]_{1,j}$	2.062	0.085	-0.031	0.011	-0.001
CI	(1.726 2.462)	(-0.040 0.214)	(-0.083 0.021)	(-0.098 0.121)	(-0.287 0.278)
$[\hat{\Sigma}_1]_{2,j}$.	1	-0.008	-0.009	0.149
CI	(. .)	(1 1)	(-0.046 0.028)	(-0.094 0.075)	(-0.060 0.368)
$[\hat{\Sigma}_1]_{3,j}$.	.	0.201	0.002	0.007
CI	(. .)	(. .)	(0.168 0.237)	(-0.039 0.041)	(-0.079 0.097)
$[\hat{\Sigma}_1]_{4,j}$.	.	.	1	0.047
CI	(. .)	(. .)	(. .)	(1 1)	(-0.144 0.248)
$[\hat{\Sigma}_1]_{5,j}$	2.151
CI	(. .)	(. .)	(. .)	(. .)	(1.532 2.908)
$[\hat{\Sigma}_2]_{1,j}$	3.23	0.04	0.581	0.862	0.882
CI	(2.719 3.793)	(-0.112 0.191)	(0.467 0.713)	(0.722 1.015)	(0.619 1.151)
$[\hat{\Sigma}_2]_{2,j}$.	1	-0.293	0.429	0.419
CI	(. .)	(1 1)	(-0.354 -0.235)	(0.361 0.492)	(0.284 0.557)
$[\hat{\Sigma}_2]_{3,j}$.	.	0.521	0.034	-0.223
CI	(. .)	(. .)	(0.438 0.617)	(-0.024 0.095)	(-0.333 -0.120)
$[\hat{\Sigma}_2]_{4,j}$.	.	.	1	0.496
CI	(. .)	(. .)	(. .)	(1 1)	(0.354 0.645)
$[\hat{\Sigma}_2]_{5,j}$	1.001
CI	(. .)	(. .)	(. .)	(. .)	(0.737 1.316)
$[\hat{\Sigma}_3]_{1,j}$	3.129	-0.762	0.38	0.623	0.834
CI	(2.684 3.620)	(-0.889 -0.633)	(0.309 0.455)	(0.469 0.775)	(0.566 1.132)
$[\hat{\Sigma}_3]_{2,j}$.	1	0.207	0.389	-0.176
CI	(. .)	(1 1)	(0.177 0.238)	(0.319 0.458)	(-0.325 -0.021)
$[\hat{\Sigma}_3]_{3,j}$.	.	0.189	0.223	0.17
CI	(. .)	(. .)	(0.164 0.216)	(0.193 0.255)	(0.108 0.240)
$[\hat{\Sigma}_3]_{4,j}$.	.	.	1	-0.337
CI	(. .)	(. .)	(. .)	(1 1)	(-0.493 -0.188)
$[\hat{\Sigma}_3]_{5,j}$	0.875
CI	(. .)	(. .)	(. .)	(. .)	(0.620 1.165)

Table 2: Simulated examples - posterior mean estimates ($\hat{\cdot}$) and 95% credible intervals (CI) of $\hat{\Sigma}_k$.

$$\lambda_1 = -5, \lambda_2 = 5, \lambda_3 = 6,$$

$$\tilde{\Sigma}_1 = \begin{bmatrix} 2 & 0 & 0.0 & 0 & 0 \\ 0 & 1 & 0.0 & 0 & 0 \\ 0 & 0 & 0.2 & 0 & 0 \\ 0 & 0 & 0.0 & 1 & 0 \\ 0 & 0 & 0.0 & 0 & 2 \end{bmatrix}, \quad \tilde{\Sigma}_2 = \begin{bmatrix} 3.000 & 0.000 & 0.551 & 0.779 & 0.857 \\ 0.000 & 1.000 & -0.318 & 0.450 & 0.495 \\ 0.551 & -0.318 & 0.500 & 0.000 & -0.318 \\ 0.779 & 0.450 & 0.000 & 1.000 & 0.450 \\ 0.857 & 0.495 & -0.318 & 0.450 & 1.000 \end{bmatrix},$$

$$\tilde{\Sigma}_3 = \begin{bmatrix} 3.000 & -0.783 & 0.377 & 0.684 & 0.781 \\ -0.783 & 1.000 & 0.214 & 0.335 & -0.092 \\ 0.377 & 0.214 & 0.200 & 0.231 & 0.209 \\ 0.684 & 0.335 & 0.231 & 1.000 & -0.382 \\ 0.781 & -0.092 & 0.209 & -0.382 & 1.000 \end{bmatrix}.$$

The marginal bivariate densities are plotted in Figure 3. We chose the parameters so to have independent (first example) and dependent variables (second and third), highly skew linear densities and, at least, one bimodal circular marginal for each example.

In the three examples inference is carried out considering 40000 iterations, burnin 30000, thin 5 and by taking 2000 posterior samples. As prior distributions we choose $\mu_k, \Sigma_k \sim \mathcal{N}(\mathbf{0}_5, 0.001, 15, \mathbf{I}_5)$ and $\lambda_k \sim \mathcal{N}_1(0, 100)$, that are standard weak informative priors. From Tables 1 and 2 we see that, with the exception of $[\hat{\mu}_2]_5$, all true values are inside the associated 95% credible intervals (CIs), proving that our algorithm is able to estimate the \mathcal{JPSN} parameters. To further corroborate the validity of the proposed MCMC scheme in solving the identification problem, in Figure 4 we show, as examples, the trace plots of parameters $[\tilde{\mu}_k]_1$, $[\tilde{\Sigma}_k]_{1,1}$ and $[\tilde{\Sigma}_k]_{1,2}$. These chains have reached their stationary distributions (we also checked it by using the R package coda [35]) with weak informative priors; this shows that the identification problem is no more relevant.

4.2. Zebras movements example

In this section we estimate the \mathcal{JPSN} parameters on an animal movement dataset taken from the movebank repository (www.movebank.org). Our aim is to show that the \mathcal{JPSN} can give information on the dependence of poly-cylindrical observations. Seven zebras are jointly observed in Botswana (Africa) between the Okavango Delta and the Makgadikgadi Pans, and their hourly positions are recorded with GPS devices during the years 2007-2009 [6]. In the observational period the zebras migrate from the dry season habitat, that is the Okavango Delta, to the rainy season habitat, that is the Makgadikgadi Pans. We select data from 4 zebras, observed between the 18 of November 2008 and the 18 of February 2009, when they have ended the migration. For each animal we compute the turning-angles and logarithm of step-lengths, having then poly-cylindrical observations composed of four circular and four linear variables. It is out of the scope of this work to introduce complex models based on the \mathcal{JPSN} , that are left to future developments, and we assume that observations are independent and identical distributed. For this reason, to mitigate temporal dependence we use data five hours apart, having then 442 observations for parameters estimate. Using the Pearson's coefficient and the circular-circular correlation of [15], i.e.,

$$\rho_{(\Theta_i, \Theta_{i'})} = \frac{E(\sin(\Theta_i - \Theta_i^*) \sin(\Theta_{i'} - \Theta_{i'}^*))}{\sqrt{E(\sin^2(\Theta_i - \Theta_i^*))E(\sin^2(\Theta_{i'} - \Theta_{i'}^*))}} \in [-1, 1], \quad (13)$$

where Θ_i^* and $\Theta_{i'}^*$ are two circular variables distributed, respectively, as Θ_i and $\Theta_{i'}$, for the subset of data used all the autocorrelations have values lower than 0.05. The histograms of the data can be seen in Figure 5.

The MCMC algorithm is implemented using the same number of iterations, thin and burnin used in the previous section while $\{\mu, \Sigma\} \sim \mathcal{N}(\mathbf{0}_{12}, 0.001, 15, \mathbf{I}_{12})$ and $\lambda \sim \mathcal{N}_4(0, 100\mathbf{I}_4)$. In Figure 5 and 6 we depicted, respectively, the marginal posterior \mathcal{JPSN} densities and the dependence matrix. The latter shows the MC estimates of the posterior mean circular-circular correlation of [15], the circular-linear dependence of [21], i.e.,

$$\rho_{(\Theta_i, Y_j)}^2 = \frac{\text{Cor}(\cos \Theta_i, Y_j)^2 + \text{Cor}(\sin \Theta_i, Y_j)^2}{1 - \text{Cor}(\cos \Theta_i, \sin \Theta_i)} + \frac{-2\text{Cor}(\cos \Theta_i, Y_j)\text{Cor}(\sin \Theta_i, Y_j)\text{Cor}(\cos \Theta_i, \sin \Theta_i)}{1 - \text{Cor}(\cos \Theta_i, \sin \Theta_i)} \in [0, 1], \quad (14)$$

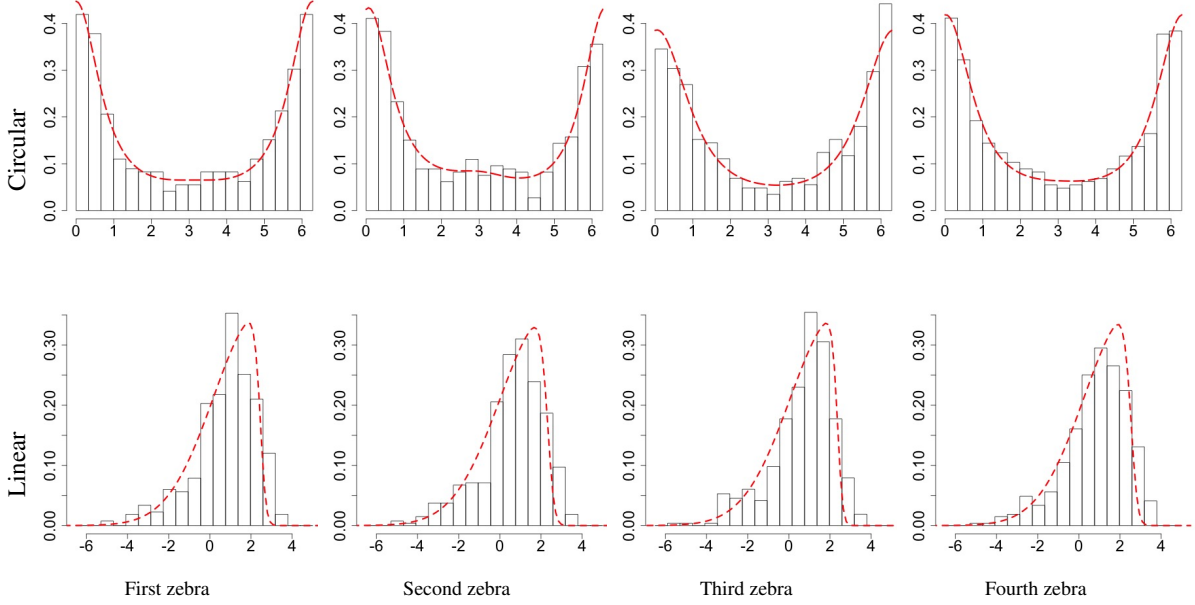


Figure 5: Zebras movement example - histograms of the observed data and posterior marginal densities of turning-angles (first row) and the logarithm of step-lengths (second row).

and linear-linear correlation, evaluated with the Pearson's coefficient. A circular-circular and linear-linear correlation is plotted only if the associated CI does not contain zero while since the CI of $\rho^2(\Theta_i, Y_j)$ has 0 probability to contain the 0, we plot the value of $\rho^2(\Theta_i, Y_j)$ using a different rationality. More precisely, since $W_i \perp Y_j$ iff $\Theta_i \perp Y_j$, in Figure 6 we plot the posterior mean value of $\rho^2(\Theta_i, Y_j)$ only if at least one of the CIs of Σ_{wy} that measure the correlation between W_i and Y_j does not contain the zero. From Figure 5 we appreciate that the \mathcal{JPSN} is able to fit satisfactorily the data and to find significant circular-linear and linear-linear correlations (Figure 6).

4.3. Comparison with cylindrical distributions

With this section we want to demonstrate that ignoring multivariate dependence leads to loss of predictive ability. Then we compare our proposal with the cylindrical distribution of Abe-Ley [1] and a cylindrical version of the \mathcal{JPSN} , i.e., for both we assume dependence between the variables belonging to the same animal and independence between zebras. Since the \mathcal{JPSN} is not available in closed form, a comparison based on informational criteria, such as AIC or BIC, is not possible. We decide to make the comparison in terms of predictive ability measured used the CRPS, that is a proper scoring rule defined for both circular [12] and linear [11] variables that measure the distance between cumulative distribution functions [29]; lower values are then preferable. The Abe-Ley distribution is defined only for a positive linear variable and then, to make a fair comparison, we use the distribution that arises by taking the logarithm of its linear component:

$$f(\theta_i, y_j) = \frac{\alpha^{AL}(\beta^{AL})^{\alpha^{AL}}}{2\pi \cosh \kappa^{AL}} \left(1 + \lambda^{AL} \sin(\theta_i - \mu^{AL})\right) e^{y_j(\alpha^{AL}-1)} e^{-(\beta^{AL} e^{y_j})^{\alpha^{AL}}} (1 - \tanh \kappa^{AL} \cos(\theta_i - \mu^{AL})) e^{y_j}.$$

$\alpha^{AL} \in \mathbb{R}^+$ and $\beta^{AL} \in \mathbb{R}^+$ are linear scale and shape parameters, $\mu^{AL} \in [0, 2\pi)$ and $\lambda^{AL} \in [-1, 1]$ endorse the role of circular location and skewness parameters and $\kappa^{AL} \in \mathbb{R}^+$ plays the role of circular concentration and circular-linear dependence parameter. For the Abe-Ley parameters we use standard weak informative priors, i.e., an inverse gamma with parameters (1,1) for α^{AL} , β^{AL} and κ^{AL} while uniform distributions on the respective domains are used for μ^{AL} and λ^{AL} . Under the cylindrical \mathcal{JPSN} , a $N_1(0, 100)$ is used for the skew parameters and a $NIW(\mathbf{0}_3, 0.001, 6, \mathbf{I}_3)$ for the others that are the marginal priors deriving from the ones of the poly-cylindrical \mathcal{JPSN} .

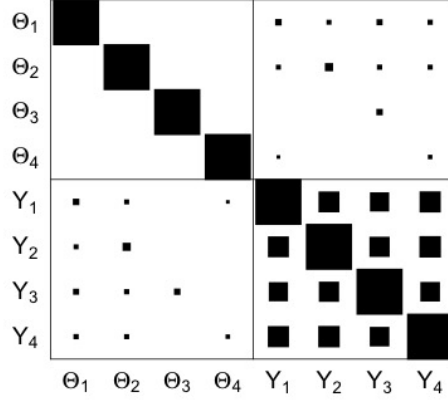


Figure 6: Zebras movement example - dependence matrix computed using equations (13) (circular-circular), (14) (circular-linear) and the Pearson's correlation coefficient (linear-linear). The size of the square is proportional to the posterior mean value. All values are positive.

We select 10% of the circular and linear observations to be set aside and not used to estimate the posterior distributions. We predict their values based on the posterior samples and we measure how the models perform in term of posterior estimates. Then, let $C_i \subset \{1, 2, \dots, T\}$ and $\mathcal{L}_j \subset \{1, \dots, T\}$ be sets of indices, where $t \in C_i$ if θ_{ti} is missing and $t \in \mathcal{L}_j$ if y_{tj} is missing, and let θ_{ti}^b , $t \in C_i$, and y_{tj}^b , $t \in \mathcal{L}_j$, be, respectively, the b^{th} posterior sample of θ_{ti} and y_{tj} . An MC approximation of the CRPS for circular variables based on B posterior samples is computed as

$$CRPS_{C_i} \approx \frac{1}{B} \sum_{b=1}^B d(\theta_{ti}, \theta_{ti}^b) - \frac{1}{2B^2} \sum_{b=1}^B \sum_{b'=1}^B d(\theta_{ti}^b, \theta_{ti}^{b'}), \quad t \in C_i,$$

where $d(\cdot, \cdot)$ is the angular distance, while the CRPS for linear variable is approximated by

$$CRPS_{\mathcal{L}_j} \approx \frac{1}{B} \sum_{b=1}^B |y_{tj} - y_{tj}^b| - \frac{1}{2B^2} \sum_{b=1}^B \sum_{b'=1}^B |y_{tj}^b - y_{tj}^{b'}|, \quad t \in \mathcal{L}_j.$$

We then compute the overall mean CRPSs for the sets of circular and linear variables and we use these indices to measure the goodness-of-fit.

Circular and linear CRPSs have values 0.383 and 0.693 for the $\mathcal{JP}SN$, 0.385 and 0.762 for the cylindrical $\mathcal{JP}SN$, and 0.412 and 0.753 for the Abe-Ley density, showing that the $\mathcal{JP}SN$ performs better and, moreover, it is also able to give a measure of dependence between all the circular and linear components (Figure 6) that is not possible with cylindrical distributions.

5. Concluding remarks

In this work we introduced a poly-cylindrical distribution. The proposal is highly flexible, it is closed under marginalization and it allows to have dependent components, bimodal marginal circular distributions and asymmetric linear ones. We showed how the MCMC algorithm, used to obtain posterior samples, can be easily implemented using only Gibbs steps. The proposal suffers from an identification problem and we showed how to overcome it with a post-processing of posterior samples that can also be used with the \mathcal{PN} distribution. With the aim to prove the validity of our sampling scheme, the algorithm was applied to simulated examples. Then the proposed distribution was used to model a real data taken from the movebank data repository. The predictive ability of our proposal was compared with the ones of cylindrical distributions, showing that the $\mathcal{JP}SN$ performs better.

Future work will lead us to use the $JPSN$ as emission distribution in an hidden Markov model and to incorporate covariates to model mean and covariance of the circular-linear observations.

Acknowledgement

The author wishes to thank Antonello Maruotti, Giovanna Jona Lasinio and Alessio Pollice for assistance and comments that greatly improved the manuscript.

This work is partially developed under the PRIN2015 supported-project Environmental processes and human activities: capturing their interactions via statistical methods (EPHASTAT) funded by MIUR (Italian Ministry of Education, University and Scientific Research).

References

References

- [1] Abe, T., Ley, C., 2017. A tractable, parsimonious and flexible model for cylindrical data, with applications. *Econometrics and Statistics* 4, 91 – 104.
- [2] Anderson-Cook, C., 1997. An extension to modeling cylindrical variables. *Statistics and Probability Letters* 35, 215 – 223.
- [3] Arellano-Valle, R., Bolfarine, H., Lachos, V., 2007. Bayesian inference for skew-normal linear mixed models. *Journal of Applied Statistics* 34, 663–682. doi:10.1080/02664760701236905.
- [4] Azzalini, A., 1985. A class of distributions which includes the normal ones. *Scandinavian Journal of Statistics* 12, 171–178.
- [5] Azzalini, A., Dalla Valle, A., 1996. The multivariate skew-normal distribution. *Biometrika* 83, 715–726. doi:10.1093/biomet/83.4.715.
- [6] Bartlam-Brooks, H.L.A., Beck, P.S.A., Bohrer, G., Harris, S., 2013. In search of greener pastures: Using satellite images to predict the effects of environmental change on zebra migration. *Journal of Geophysical Research: Biogeosciences* 118, 1427–1437. doi:10.1002/jgrg.20096.
- [7] Brooks, S., Gelman, A., Jones, G., Meng, X., 2011. *Handbook of Markov Chain Monte Carlo*. Chapman & Hall/CRC Handbooks of Modern Statistical Methods, CRC Press.
- [8] Bulla, J., Lagona, F., Maruotti, A., Picone, M., 2012. A multivariate hidden Markov model for the identification of sea regimes from incomplete skewed and circular time series. *Journal of Agricultural, Biological, and Environmental Statistics* 17, 544–567. doi:10.1007/s13253-012-0110-1.
- [9] D’Elia, A., 2001. A statistical model for orientation mechanism. *Statistical Methods and Applications* 10, 157–174. doi:10.1007/BF02511646.
- [10] Gatto, R., Jammalamadaka, S.R., 2007. The generalized von mises distribution. *Statistical Methodology* 4, 341 – 353. doi:http://dx.doi.org/10.1016/j.stamet.2006.11.003.
- [11] Gneiting, T., Raftery, A.E., 2007. Strictly proper scoring rules, prediction, and estimation. *Journal of the American Statistical Association* 102, 359–378.
- [12] Gritti, E.P., Gneiting, T., Berrocal, V.J., Johnson, N.A., 2006. The continuous ranked probability score for circular variables and its application to mesoscale forecast ensemble verification. *Quarterly Journal of the Royal Meteorological Society* 132, 2925–2942. doi:10.1256/qj.05.235.
- [13] Gupta, A.K., González-Farías, G., Domínguez-Molina, J., 2004. A multivariate skew normal distribution. *Journal of Multivariate Analysis* 89, 181 – 190. doi:http://dx.doi.org/10.1016/S0047-259X(03)00131-3.
- [14] Hernandez-Stumpfhauser, D., Breidt, F.J., van der Woerd, M.J., 2016. The general projected normal distribution of arbitrary dimension: modeling and Bayesian inference. *Bayesian Analysis* doi: 10.1214/15-BA989.
- [15] Jammalamadaka, S., Sarma, Y., 1988. A correlation coefficient for angular variables. *Statistical Theory and Data Analysis II*, 349–364.
- [16] Jammalamadaka, S.R., SenGupta, A., 2001. *Topics in Circular Statistics*. World Scientific, Singapore.
- [17] Johnson, R.A., Wehrly, T.E., 1978. Some angular-linear distributions and related regression models. *Journal of the American Statistical Association* 73, 602–606.
- [18] Jones, M.C., Pewsey, A., 2009. Sinh-arcsinh distributions. *Biometrika* 96, 761–780.
- [19] Jonsen, I.D., Flemming, J.M., Myers, R.A., 2005. Robust state-space modeling of animal movement data. *Ecology* 86, 2874–2880.
- [20] Lagona, F., Picone, M., 2011. A latent-class model for clustering incomplete linear and circular data in marine studies. *Journal of Data Science* 9.
- [21] Mardia, K.V., 1976. Linear-circular correlation coefficients and rhythmometry. *Biometrika* 63.
- [22] Mardia, K.V., Jupp, P.E., 1999. *Directional Statistics*. John Wiley and Sons, Chichester.
- [23] Mardia, K.V., Sutton, T.W., 1978. A model for cylindrical variables with applications. *Journal of the Royal Statistical Society. Series B (Methodological)* 40, 229–233.
- [24] Maruotti, A., Punzo, A., Mastrantonio, G., Lagona, F., 2015. A time-dependent extension of the projected normal regression model for longitudinal circular data based on a hidden Markov heterogeneity structure. *Stochastic Environmental Research and Risk Assessment* To appear.
- [25] Mastrantonio, G., Calise, G., 2016. Hidden Markov model for discrete circular-linear wind data time series. *Journal of Statistical Computation and Simulation* To appear. doi:10.1080/00949655.2016.1142544.
- [26] Mastrantonio, G., Jona Lasinio, G., Gelfand, A.E., 2015a. Spatio-temporal circular models with non-separable covariance structure. *TEST* To appear. doi:10.1007/s11749-015-0458-y.

- [27] Mastrantonio, G., Jona Lasinio, G., Maruotti, A., Calise, G., 2017. Invariance properties and statistical inference for circular data. *Statistica Sinica* To appear.
- [28] Mastrantonio, G., Maruotti, A., Jona Lasinio, G., 2015b. Bayesian hidden Markov modelling using circular-linear general projected normal distribution. *Environmetrics* 26, 145–158.
- [29] Matheson, J.E., Winkler, R.L., 1976. Scoring rules for continuous probability distributions. *Management Science* 22, 1087–1096.
- [30] Morales, J.M., Haydon, D.T., Frair, J., Holsinger, K.E., Fryxell, J.M., 2004. Extracting more out of relocation data: building movement models as mixtures of random walks. *Ecology* 85, 2436–2445.
- [31] Morales, J.M., Moorcroft, P.R., Matthiopoulos, J., Frair, J.L., Kie, J.G., Powell, R.A., Merrill, E.H., Haydon, D.T., 2010. Building the bridge between animal movement and population dynamics. *Philosophical Transactions of the Royal Society B: Biological Sciences* 365, 2289–2301. doi:10.1098/rstb.2010.0082.
- [32] Olmos, N.M., Varela, H., Gómez, H.W., Bolfarine, H., 2012. An extension of the half-normal distribution. *Statistical Papers* 53, 875–886. doi:10.1007/s00362-011-0391-4.
- [33] Patterson, T., Thomas, L., Wilcox, C., Ovaskainen, O., Matthiopoulos, J., 2008. State-space models of individual animal movement. *Trends in Ecology & Evolution* 23, 87–94.
- [34] Pewsey, A., Neuhaus, M., Ruxton, G.D., 2013. *Circular Statistics in R*. Oxford University Press, Croydon.
- [35] Plummer, M., Best, N., Cowles, K., Vines, K., 2006. Coda: Convergence diagnosis and output analysis for mcmc. *R News* 6, 7–11.
- [36] Robert, C.P., Casella, G., 2005. *Monte Carlo Statistical Methods* (Springer Texts in Statistics). Springer-Verlag New York, Inc., Secaucus, NJ, USA.
- [37] Sahu, S.K., Dey, D.K., Branco, M.D., 2003. A new class of multivariate skew distributions with applications to Bayesian regression models. *Canadian Journal of Statistics* 31, 129–150.
- [38] Storch, K.F., Lipan, O., Leykin, I., Viswanathan, N., Davis, F.C., Wong, W.H., Weitz, C.J., 2002. Extensive and divergent circadian gene expression in liver and heart. *Nature* 417, 78–83.
- [39] Wang, F., Gelfand, A., Jona Lasinio, G., 2015. Joint spatio-temporal analysis of a linear and a directional variable: space-time modeling of wave heights and wave directions in the Adriatic sea. *Statistica Sinica* 25, 25–39. doi:10.5705/ss.2013.204w.
- [40] Wang, F., Gelfand, A.E., 2013. Directional data analysis under the general projected normal distribution. *Statistical Methodology* 10, 113–127.
- [41] Wang, F., Gelfand, A.E., 2014. Modeling space and space-time directional data using projected Gaussian processes. *Journal of the American Statistical Association* 109, 1565–1580. doi:10.1080/01621459.2014.934454.

Appendix

A. The invariance property of the \mathcal{PN}

Here we prove that the univariate marginal density of the circular variables is invariant. Let $\Theta_i^* = \delta(\Theta_i + \xi)$, where $\delta \in \{-1, 1\}$ and $\xi \in [0, 2\pi)$, following Theorem 1 of [27], the density of $\Theta_i \sim \mathcal{PN}_1(\mu_{w_i}, \Sigma_{w_i})$, i.e., $f_{\Theta_i}(\cdot)$, has the invariant property if $f_{\Theta_i^*}(\cdot)$, i.e., the density of Θ_i^* , belongs to the same parametric family of $f_{\Theta_i}(\cdot)$.

The random variables Θ_i^* can be written as

$$\Theta_i^* = \text{atan}^* \frac{\sin \Theta_i^*}{\cos \Theta_i^*} = \text{atan}^* \frac{\sin(\delta(\Theta_i + \xi))}{\cos(\delta(\Theta_i + \xi))} = \text{atan}^* \frac{\delta \sin(\Theta_i + \xi)}{\cos(\Theta_i + \xi)}, \quad (\text{A.1})$$

and using relations $\cos(\alpha + \beta) = \cos \alpha \cos \beta - \sin \alpha \sin \beta$ and $\sin(\alpha + \beta) = \sin \alpha \cos \beta + \cos \alpha \sin \beta$, equation (A.1) can be stated equivalently as

$$\Theta_i^* = \text{atan}^* \frac{\delta(R_i \sin \Theta_i \cos \xi + R_i \cos \Theta_i \sin \xi)}{R_i \cos \Theta_i \cos \xi - R_i \sin \Theta_i \sin \xi} = \text{atan}^* \frac{\delta(W_{i2} \cos \xi + W_{i1} \sin \xi)}{W_{i1} \cos \xi - W_{i2} \sin \xi}.$$

To prove that Θ_i^* is \mathcal{PN} distributed, let consider the random variable $\mathbf{W}_i^* = \Delta \mathbf{T} \mathbf{W}_i$, where $\Delta = \text{diag}((1, \delta)^\top)$ and

$$\mathbf{T} = \begin{pmatrix} \cos \xi & -\sin \xi \\ \sin \xi & \cos \xi \end{pmatrix}.$$

\mathbf{W}_i^* is normally distributed and equation (1) applied to \mathbf{W}_i^* gives

$$\text{atan}^* \frac{W_{i2}^*}{W_{i1}^*} = \text{atan}^* \frac{\delta(W_{i2} \cos \xi + W_{i1} \sin \xi)}{W_{i1} \cos \xi - W_{i2} \sin \xi} = \Theta_i^*.$$

Then Θ_i^* follows a projected normal distribution; this proves the invariance of the \mathcal{PN} .

B. MCMC implementation details

Sampling μ and Σ . The full conditional of $\{\mu, \Sigma\}$ is proportional to

$$\prod_{t=1}^T \phi_{2p+q}((\mathbf{w}_t, \mathbf{y}_t)^\top - (\mathbf{0}_{2p}, \text{diag}(\lambda)\mathbf{d}_t)^\top | \mu, \Sigma) f(\mu, \Sigma | \lambda). \quad (\text{B.2})$$

Equation (B.2) is equivalent to the full conditional of the mean and covariance matrix in a model with i.i.d. normally distributed observations. If we assume $f(\mu, \Sigma | \lambda) \equiv f(\mu, \Sigma)$, with

$$f(\mu, \Sigma) \propto |\Sigma|^{-(\nu_0 + 2p + q)/2 - 1} \exp \left(-\frac{\text{tr}(\Psi_0 \Sigma^{-1}) + \kappa_0 (\mu - \mu_0)^\top \Sigma^{-1} (\mu - \mu_0)}{2} \right)$$

i.e., $f(\mu, \Sigma)$ is the density of a $\mathcal{N}\mathcal{I}\mathcal{W}(\mu_0, \kappa_0, \nu_0, \Psi_0)$, where $\kappa_0 > 0$ and $\nu_0 > 2p + q - 1$ are real numbers, $\mu_0 \in \mathbb{R}^{2p+q}$ and Ψ_0 is a $(2p + q) \times (2p + q)$ nnd matrix, and we let $\eta_t = (\mathbf{w}_t, \mathbf{y}_t)^\top - (\mathbf{0}_{2p}, \text{diag}(\lambda)\mathbf{d}_t)^\top$ and

$$\bar{\eta} = \frac{1}{T} \sum_{t=1}^T \eta_t,$$

the full conditional is $\mathcal{N}\mathcal{I}\mathcal{W}(\mu_{\text{post}}, \kappa_{\text{post}}, \nu_{\text{post}}, \Psi_{\text{post}})$ with

$$\begin{aligned} \mu_{\text{post}} &= \frac{\kappa_0 \mu_0 + T \bar{\eta}}{\kappa_0 + T}, \\ \kappa_{\text{post}} &= \kappa_0 + T, \\ \nu_{\text{post}} &= \nu_0 + T, \\ \Psi_{\text{post}} &= \Psi_0 + \sum_{t=1}^T (\eta_t - \bar{\eta})(\eta_t - \bar{\eta})^\top + \frac{\kappa_0 T}{\kappa_0 + T} (\bar{\eta} - \mu_0)(\bar{\eta} - \mu_0)^\top. \end{aligned}$$

Sampling λ . The full conditional of λ is proportional to

$$\prod_{t=1}^T \phi_q(\mathbf{y}_t | \mu_{y_t | w_t} + \text{diag}(\mathbf{d}_t) \lambda, \Sigma_{y|w}) g_2(\lambda), \quad (\text{B.3})$$

where $\mu_{y_t | w_t} = \mu_y + \Sigma_{wy}^\top \Sigma_w^{-1} (\mathbf{w}_t - \mu_w)$ and $\Sigma_{y|w} = \Sigma_y - \Sigma_{wy}^\top \Sigma_w^{-1} \Sigma_{wy}$. In (B.3) we can see λ as a vector of regression coefficients, where the matrix of covariates is $\text{diag}(\mathbf{d}_t)$. Then, standard results tell us that a normal $g_2(\lambda)$ induces a normal full conditional. More precisely, let $\lambda \sim \mathcal{N}_q(\gamma_0, \Omega_0)$, then the full conditional is $\mathcal{N}_q(\gamma_{\text{post}}, \Omega_{\text{post}})$ with

$$\begin{aligned} \Omega_{\text{post}} &= \left(\sum_{t=1}^T \text{diag}(\mathbf{d}_t) \Sigma_{y|w}^{-1} \text{diag}(\mathbf{d}_t) + \Omega_0^{-1} \right)^{-1}, \\ \gamma_{\text{post}} &= \Omega_{\text{post}} \left(\sum_{t=1}^T \text{diag}(\mathbf{d}_t) \Sigma_{y|w}^{-1} (\mathbf{y}_t - \mu_{y_t | w_t}) + \Omega_0^{-1} \gamma_0 \right). \end{aligned}$$

Sampling \mathbf{D}_t . The full conditional of the latent vector \mathbf{D}_t is proportional to

$$\phi_q(\mathbf{y}_t | \mu_{y_t | w_t} + \text{diag}(\lambda) \mathbf{d}_t, \Sigma_{y|w}) \phi_q(\mathbf{d}_t | \mathbf{0}_q, \mathbf{I}_q).$$

\mathbf{d}_t can be seen as a vector of (positive) regressors with $\text{diag}(\lambda)$ as matrix of covariates and $\phi_q(\mathbf{d}_t | \mathbf{0}_q, \mathbf{I}_q)$ as prior. The full conditional is then $N_q(\mathbf{M}_{d_t}, \mathbf{V}_q) I_{0_q, \infty}$, where $N_q(\cdot, \cdot) I_{0_q, \infty}$ is a q -dimensional truncated normal distribution with components having support \mathbb{R}^+ ,

$$\mathbf{V}_d = (\Lambda^\top \Sigma_{y|w}^{-1} \Lambda + \mathbf{I}_q)^{-1}$$

and

$$\mathbf{M}_{d_t} = \mathbf{V}_d \Lambda^\top \Sigma_{y|w}^{-1} (\mathbf{y}_t - \mu_{y_t | w_t}).$$

Sampling R_{ti} . Let $\mathbf{u}_{ti} = (\cos \theta_{ti}, \sin \theta_{ti})^\top$, $A_{ti} = \mathbf{u}_{ti}^\top \Sigma_{w_{ti}|w_{t-i}, y_t}^{-1} \mathbf{u}_{ti}$ and $B_{ti} = \mathbf{u}_{ti}^\top \Sigma_{w_{ti}|w_{t-i}, y_t}^{-1} \boldsymbol{\mu}_{w_{ti}|w_{t-i}, y_t}$, where $\boldsymbol{\mu}_{w_{ti}|w_{t-i}, y_t}$ and $\Sigma_{w_{ti}|w_{t-i}, y_t}$ are the conditional mean and covariance matrix of \mathbf{w}_{ti} assuming $(\mathbf{w}_t, \mathbf{y}_t)^\top \sim \mathcal{N}_{2p+q}(\boldsymbol{\mu} + (\mathbf{0}_{2p}, \text{diag}(\lambda)\mathbf{d}_t)^\top, \Sigma)$. The full conditional of R_{ti} is then proportional to

$$r_{ti} \exp\left(-\frac{1}{2}A_{ti}\left(r_{ti} - \frac{B_{ti}}{A_{ti}}\right)^2\right). \quad (\text{B.4})$$

Equation (B.4) is the same full conditional of the latent variable of the spherical \mathcal{PN} of [14] and then we can use their *slice sampling* strategy to sample from it.

In details, if

$$\begin{aligned} v_{ti} &\sim \mathcal{U}\left(0, \exp\left(-\frac{1}{2}A_{ti}\left(r_{ti} - \frac{B_{ti}}{A_{ti}}\right)^2\right)\right), \\ v_{ti}^* &\sim \mathcal{U}(0, 1), \end{aligned}$$

then

$$r_{ti} = \sqrt{(\varrho_{2ti}^2 - \varrho_{1ti}^2)v_{ti}^* + \varrho_{1ti}^2},$$

with

$$\begin{aligned} \varrho_{1ti} &= \frac{B_{ti}}{A_{ti}} + \max\left\{-\frac{B_{ti}}{A_{ti}}, -\sqrt{\frac{-2 \ln v_{ti}}{A_{ti}}}\right\}, \\ \varrho_{2ti} &= \frac{B_{ti}}{A_{ti}} + \sqrt{\frac{-2 \ln v_{ti}}{A_{ti}}}, \end{aligned}$$

is distributed accordingly to the full conditional (B.4).

The joint projected normal and skew-normal: a distribution for poly-cylindrical data

Gianluca Mastrantonio

Department of Mathematical Science, Polytechnic of Turin, Corso Duca degli Abruzzi,
24, 10129 Turin Italy

Abstract

The contribution of this work is the introduction of a multivariate circular-linear (or poly-cylindrical) distribution obtained by combining the projected and the skew-normal. We show the flexibility of our proposal, its property of closure under marginalization and how to quantify multivariate dependence.

Due to a non-identifiability issue that our proposal inherits from the projected normal, a computational problem arises. We overcome it in a Bayesian framework, adding suitable latent variables and showing that posterior samples can be obtained with a post-processing of the estimation algorithm output. Under specific prior choices, this approach enables us to implement a Markov chain Monte Carlo algorithm relying only on Gibbs steps, where the updates of the parameters are done as if we were working with a multivariate normal likelihood. The proposed approach can be also used with the projected normal.

As a proof of concept, on simulated examples we show the ability of our algorithm in recovering the parameters values and to solve the identification problem. Then the proposal is used in a real data example, where the turning-angles (circular variables) and the logarithm of the step-lengths (linear variables) of four zebras are jointly modelled.

1 Introduction

The analysis of circular data, i.e., observations with support the unit circle, requires specific statistical tools since the circular domain is intrinsically different from the real line, that is the domain of linear variables, and this inhibits the use of standard statistics that if not properly modified lead to not interpretable results; for a general review see Jammalamadaka and SenGupta (2001), Mardia and Jupp (1999) or Pewsey et al. (2013). A similar type of problem holds for circular densities that, besides being non negative and to integrate to 1, should possess the property of “invariance” (Mastrantonio et al., 2017), i.e., they must be a location model under the group of rotations and reflections of the circle. This property, that expresses the need of densities that can represent equivalently the same phenomena under different reference systems, is peculiar of circular densities and it is sometimes overlooked (Mastrantonio et al., 2017).

Circular data are often observed along with linear ones and they are called cylindrical if bivariate, otherwise poly-cylindrical. For example in marine research wind and wave directions are modelled with wind speed and wave height (Bulla et al., 2012; Wang et al., 2015; Mastrantonio and Calise, 2016) and, in ecology, animal behaviour is described using measures of speed and direction, e.g., step-length and turning-angle (D’Elia, 2001; Jonsen et al., 2005; Patterson et al., 2008; Morales et al., 2010). In most of the applications cylindrical data are modelled assuming independence between the circular and linear components, see for example Bulla et al. (2012), Lagona and Picone (2011) or Morales et al. (2004). Ignoring dependence can lead to misleading inference since we are not considering a component of the data that can help in understanding the phenomenon under study (see for example

Mastrantonio et al., 2015b). In the literature, to date, no poly-cylindrical distributions have been proposed and there are only few distributions for cylindrical data; the best known examples are the ones of Anderson-Cook (1997), Johnson and Wehrly (1978), Mardia and Sutton (1978) and the new density of Abe and Ley (2017). The aim of this work is to introduce what is, to the best of our knowledge, the first poly-cylindrical distribution.

Circular and linear variables live in very different spaces and the definition of a mixed-domain distribution is not easy. The issue is even more complicated if we require flexibility, interpretable parameters and the possibility to define an efficient and easy to implement estimation algorithm. We decide to put ourself in a Bayesian framework because, as we show in Section 3.1, using standard Markov chain Monte Carlo (MCMC) methods we are able to propose an algorithm with the required characteristics while Monte Carlo (MC) procedures (Brooks et al., 2011; Robert and Casella, 2005) allow us to obtain posterior distributions for all the statistics we may need to describe the results.

Since circular observations show often bimodality, see for example Storch et al. (2002) or Wang and Gelfand (2013), our aim is to propose a distribution with circular marginals that can model such data. In the literature the most known bimodal circular distributions are the projected normal (\mathcal{PN}) (Wang and Gelfand, 2013) and the generalized von Mises (Gatto and Jammalamadaka, 2007). The former can be easily generalized to the multivariate setting and it has an interesting augmented density representation, based on a normal probability density function (pdf), that can be used to define circular-linear dependence. The \mathcal{PN} is very flexible (see for example Wang and Gelfand, 2014; Mastrantonio et al., 2015a) with shapes that range from unimodal and symmetric to bimodal and antipodal, it is closed under marginalization and, as we show in the Appendix, it has the invariance property. On the other hand, multivariate extensions of the generalized von Mises are not easy to handle and, in our opinion, it not straightforward to use it as a component of a poly-cylindrical distribution.

We define our proposal constructively, starting from the \mathcal{PN} and choosing a distribution for the linear component that, taking advantage of the \mathcal{PN} augmented density representation, allows us to define a poly-cylindrical distribution whose parameters can be easily estimated with MCMC algorithms and it is flexible enough to model real data.

For the linear component we use a skew-normal, that is a generalization of the Gaussian distribution which allows more flexibility introducing asymmetry in the normal density. Its first univariate version was proposed by Azzalini (1985) and following works introduced multivariate extensions and different formalizations; see for example Azzalini and Dalla Valle (1996), Gupta et al. (2004), Jones and Pewsey (2009) or Sahu et al. (2003). Among these, we found the one of Sahu et al. (2003) (hereafter \mathcal{SSN}) interesting: it can be closed under marginalization and it has an augmented density representation that, as the \mathcal{PN} , is based on a normal pdf.

Using this particular form of the skew-normal distribution, due to the properties listed above, we are able to define the *joint projected normal and skew-normal* (\mathcal{JPSN}) poly-cylindrical distribution by introducing dependence in the normal pdfs of the augmented representations. The distribution retains the \mathcal{PN} and \mathcal{SSN} as marginal distributions and is closed under marginalization, i.e., any subset of circular and linear variables is \mathcal{JPSN} distributed. The MCMC algorithm we propose can be based only on Gibbs steps, updating parameters as if we were working with a multivariate normal likelihood. The density cannot be expressed in closed form but, from the point of view of model fitting, since we are able to estimate its parameters easily we do not consider this an issue.

The \mathcal{JPSN} has the same identification problem of the \mathcal{PN} (Wang and Gelfand, 2013), but we show that posterior values can be obtained by a post-processing of the MCMC algorithm based on the non-identifiable likelihood. The proposed algorithm can be also used with the univariate and multivariate \mathcal{PN} and the spherical \mathcal{PN} distribution of Hernandez-Stumpfhauser et al. (2016), solving their identification problem in a new way.

The algorithm, tested on simulated datasets, shows its ability in retrieving the parameters used to simulate the data and posterior samples do not suffer from an identification issue. We used the \mathcal{JPSN} to jointly model the logarithm of step-lengths and turning-angles of 4 zebras observed in Botswana (Africa). A comparison based on the continuous rank probability scores (CRPSs) Gneiting and Raftery (2007); Gritti et al. (2006) between our proposal, the cylindrical distribution of Abe and

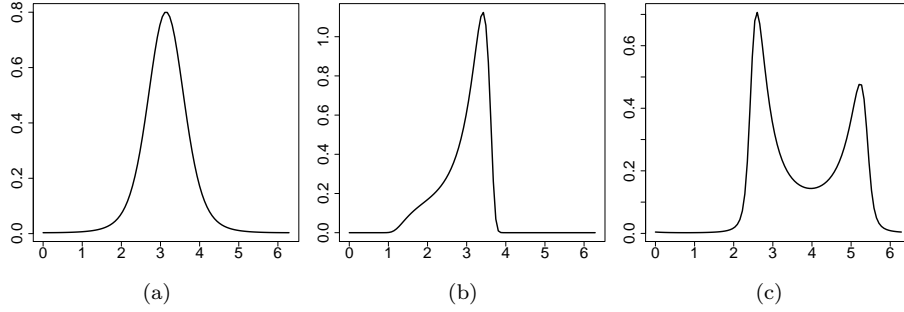


Figure 1: Univariate projected normal densities under three sets of parameters: (a) $\boldsymbol{\mu}_{w_i} = \begin{pmatrix} 2 \\ 0 \end{pmatrix}$, $\boldsymbol{\Sigma}_{w_i} = \begin{pmatrix} 1 & 0 \\ 0 & 1 \end{pmatrix}$; (b) $\boldsymbol{\mu}_{w_i} = \begin{pmatrix} 2 \\ 0 \end{pmatrix}$, $\boldsymbol{\Sigma}_{w_i} = \begin{pmatrix} 1 & 0.9 \\ 0.9 & 1 \end{pmatrix}$; (c) $\boldsymbol{\mu}_{w_i} = \begin{pmatrix} -0.1 \\ -0.2 \end{pmatrix}$, $\boldsymbol{\Sigma}_{w_i} = \begin{pmatrix} 1 & -0.9 \\ -0.9 & 1 \end{pmatrix}$

Ley (2017) and a cylindrical version of the \mathcal{JPNS} , i.e., assuming independence between zebras, is provided, showing that ignoring multivariate dependence can lead to loss of predictive ability.

The paper is organized as follows. Section 2 is devoted to the constructive definition of the distribution. In Section 3 we introduce the identification problem and how to estimate the \mathcal{JPNS} parameters. The proposal is applied to simulated examples in Section 4.1 and the real data application is shown in Section 4.2. The paper ends with concluding remarks in Section 5. In the Appendix we prove the invariance property of the \mathcal{PN} and we show MCMC implementation details.

2 The joint projected normal and skew-normal distribution

In this section we build the poly-cylindrical density by first introducing the circular and linear marginals and then showing how to induce dependence.

2.1 The projected normal distribution

The \mathcal{PN} is a distribution for a p -dimensional vector $\boldsymbol{\Theta} = \{\Theta_i\}_{i=1}^p$ of circular variables, i.e., $\Theta_i \in [0, 2\pi)$ is an angle expressed in radian, obtained starting from a $2p$ -dimensional vector $\mathbf{W} = \{\mathbf{W}_i\}_{i=1}^p$, where $\mathbf{W}_i = (W_{i1}, W_{i2})^\top \in \mathbb{R}^2$, distributed as a $2p$ -variate normal with mean vector $\boldsymbol{\mu}_w$ and covariance matrix $\boldsymbol{\Sigma}_w$. \mathbf{W}_i , normally distributed with parameters $\{\boldsymbol{\mu}_{w_i}, \boldsymbol{\Sigma}_{w_i}\}$, is a point in the 2-dimensional space expressed using the Cartesian system. The same point can be also represented in polar coordinates with the angle Θ_i and the distance vector $R_i \in \mathbb{R}^+$. Between \mathbf{W}_i , Θ_i and R_i the following relations exist:

$$\Theta_i = \text{atan}^* \left(\frac{W_{i2}}{W_{i1}} \right) \quad (1)$$

and

$$\mathbf{W}_i = R_i \begin{pmatrix} \cos \Theta_i \\ \sin \Theta_i \end{pmatrix}, \quad R_i = \|\mathbf{W}_i\|,$$

where

$$\text{atan}^* \left(\frac{S}{C} \right) = \begin{cases} \text{atan} \left(\frac{S}{C} \right) & \text{if } C > 0, S \geq 0, \\ \frac{\pi}{2} & \text{if } C = 0, S > 0, \\ \text{atan} \left(\frac{S}{C} \right) + \pi & \text{if } C < 0, \\ \text{atan} \left(\frac{S}{C} \right) + 2\pi & \text{if } C \geq 0, S < 0, \\ \text{undefined} & \text{if } C = 0, S = 0, \end{cases}$$

is a modified arctangent function used to define a quadrant-specific inverse of the tangent.

If we transform each \mathbf{W}_i in $(\Theta_i, R_i)^\top$ the Jacobian of the transformation is $\prod_{i=1}^p R_i$ and then the joint density of $(\boldsymbol{\Theta}, \mathbf{R})^\top$, where $\mathbf{R} = \{R_i\}_{i=1}^p$, is given by

$$f(\boldsymbol{\theta}, \mathbf{r}) = \prod_{i=1}^p r_i \phi_{2p}(\mathbf{w} | \boldsymbol{\mu}_w, \boldsymbol{\Sigma}_w), \quad (2)$$

where $f(\cdot)$ indicates the density of its arguments, \mathbf{r} is a realization of \mathbf{R} , $\phi_{2p}(\mathbf{w} | \boldsymbol{\mu}_w, \boldsymbol{\Sigma}_w)$ is the pdf evaluated at \mathbf{w} of a $2p$ -variate normal distribution with mean $\boldsymbol{\mu}_w$ and covariance matrix $\boldsymbol{\Sigma}_w$; here \mathbf{w} must be seen as a function of $(\boldsymbol{\theta}, \mathbf{r})^\top$.

The marginal density of $\boldsymbol{\Theta}$, obtained by integrating out \mathbf{R} in (2), is a p -variate projected normal with parameters $\boldsymbol{\mu}_w$ and $\boldsymbol{\Sigma}_w$, i.e., $\boldsymbol{\Theta} \sim \mathcal{PN}_p(\boldsymbol{\mu}_w, \boldsymbol{\Sigma}_w)$. As shown in Wang and Gelfand (2013), the \mathcal{PN} can be symmetric, asymmetric and bimodal; univariate shapes are depicted in Figure 1.

A closed form expression for the \mathcal{PN}_p density is only available in the univariate case ($p = 1$) and it is

$$f(\theta_i) = \frac{\phi_2(\boldsymbol{\mu}_{w_i} | \mathbf{0}_2, \boldsymbol{\Sigma}_{w_i}) + |\boldsymbol{\Sigma}_{w_i}|^{-1} D(\theta_i) \Phi_1(D(\theta_i) | 0, 1) \phi_1(|\boldsymbol{\Sigma}_{w_i}|^{-1} C(\theta_i)^{-1/2} (\mu_{w_{i1}} \sin \theta_i - \mu_{w_{i2}} \cos \theta_i))}{C(\theta_i)},$$

where

$$\begin{aligned} C(\theta_i) &= |\boldsymbol{\Sigma}_{w_i}|^{-2} (\sigma_{w_{i2}}^2 \cos^2 \theta_i - \rho_{w_i} \sigma_{w_{i1}} \sigma_{w_{i2}} \sin 2\theta_i + \sigma_{w_{i1}}^2 \sin^2 \theta_i), \\ D(\theta_i) &= \frac{|\boldsymbol{\Sigma}_{w_i}|^{-2} (\mu_{w_{i1}} \sigma_{w_{i2}} (\sigma_{w_{i2}} \cos \theta_i - \rho_{w_i} \sigma_{w_{i1}} \sin \theta_i) + \mu_{w_{i2}} \sigma_{w_{i1}} (\sigma_{w_{i1}} \sin \theta_i - \rho_{w_i} \sigma_{w_{i2}} \cos \theta_i))}{\sqrt{C(\theta_i)}}, \end{aligned}$$

$\Phi_\ell(\cdot | \cdot, \cdot)$ indicates the normal ℓ -variate cumulative distribution function with given mean vector and covariance matrix, $\mathbf{0}_\ell$ is a vector of 0s of length ℓ , $\mu_{w_{ij}}$ and $\sigma_{w_{ij}}^2$ are the mean and variance of W_{ij} and ρ_{w_i} is the correlation between W_{i1} and W_{i2} .

In practical applications (see for example Wang and Gelfand, 2014; Mastrantonio et al., 2015a; Maruotti et al., 2015) it is generally preferable to work with the pair $(\boldsymbol{\Theta}, \mathbf{R})^\top$ that has the nice closed form density given in equation (2), treating \mathbf{R} as a vector of latent variables.

The multivariate \mathcal{PN} is closed under marginalization since $\boldsymbol{\Theta}_A \sim \mathcal{PN}_{n_A}(\boldsymbol{\mu}_{w,A}, \boldsymbol{\Sigma}_{w,A})$, where $A \subset \{1, \dots, p\}$, n_A indicates the cardinality of the set A and $\{\boldsymbol{\mu}_{w,A}, \boldsymbol{\Sigma}_{w,A}\}$ are mean and covariance matrix of \mathbf{W}_A . Moreover, as we show in Appendix A, the univariate \mathcal{PN} posses the invariance property and then inference does not depend on the reference system chosen for the circular variables (Mastrantonio et al., 2017).

2.2 The skew-normal distribution

We now introduce the skew-normal distribution of Sahu et al. (2003) as the distribution of a q -dimensional vector $\mathbf{Y} = \{Y_j\}_{j=1}^q$, with $Y_j \in \mathbb{R}$. Let $\boldsymbol{\mu}_y$ be a vector of length q , $\boldsymbol{\Sigma}_y$ be a $q \times q$ non-negative definite (nnd) matrix and $\boldsymbol{\Lambda} = \text{diag}(\boldsymbol{\lambda})$ be a $q \times q$ diagonal matrix with diagonal elements $\boldsymbol{\lambda} = \{\lambda_i\}_{i=1}^q \in \mathbb{R}^q$. We say that \mathbf{Y} is distributed accordingly to a q -variate skew-normal with parameters $\boldsymbol{\mu}_y$, $\boldsymbol{\Sigma}_y$ and $\boldsymbol{\lambda}$ ($\mathbf{Y} \sim \mathcal{SSN}_q(\boldsymbol{\mu}_y, \boldsymbol{\Sigma}_y, \boldsymbol{\lambda})$) if it has pdf

$$f(\mathbf{y}) = 2^q \phi_q(\mathbf{y} | \boldsymbol{\mu}_y, \boldsymbol{\Upsilon}) \Phi_q\left(\boldsymbol{\Lambda}^\top \boldsymbol{\Upsilon}^{-1}(\mathbf{y} - \boldsymbol{\mu}_y) | \mathbf{0}_q, \boldsymbol{\Gamma}\right), \quad (3)$$

where $\boldsymbol{\Upsilon} = \boldsymbol{\Sigma}_y + \boldsymbol{\Lambda} \boldsymbol{\Lambda}^\top$, $\boldsymbol{\Gamma} = \mathbf{I}_q - \boldsymbol{\Lambda}^\top \boldsymbol{\Upsilon}^{-1} \boldsymbol{\Lambda}$ and \mathbf{I}_q is the identity matrix of dimension q . Although in Sahu et al. (2003) $\boldsymbol{\Lambda}$ is defined as a full matrix, here we constrain it to be diagonal to have a \mathcal{SSN} closed under marginalization; the same property will be inherited by our poly-cylindrical distribution

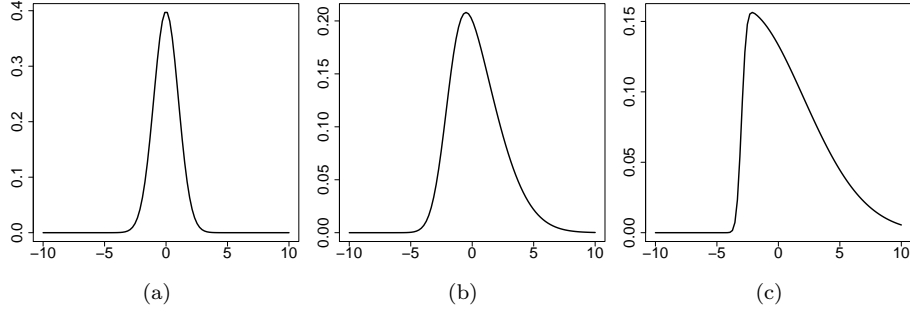


Figure 2: Univariate skew-normal densities under three sets of parameters: (a) $\mu_y = 0$, $\Sigma_y = 1$, $\lambda = 0$; (b) $\mu_y = -2$, $\Sigma_y = 1$, $\lambda = 3$; (c) $\mu_y = -3$, $\Sigma_y = 0.1$, $\lambda = 5$.

(see Section 2.3). From (3) we clearly see that $\mathbf{Y} \sim \mathcal{N}_q(\mu_y, \Sigma_y)$ if Λ is a null matrix and for this reason it is called the *skewness parameter*. Examples of univariate \mathcal{SSN} densities are shown in Figure 2.

The \mathcal{SSN} has a nice stochastic representation (Arellano-Valle et al., 2007) that is useful for the definition of the poly-cylindrical distribution. Let $\mathbf{D} \sim \mathcal{HN}_q(\mathbf{0}_q, \mathbf{I}_q)$, where $\mathcal{HN}_q(\cdot, \cdot)$ indicates the q -dimensional half normal (Olmos et al., 2012), and $\mathbf{H} \sim \mathcal{N}_q(\mathbf{0}_q, \Sigma_y)$, then \mathbf{Y} can be written as

$$\mathbf{Y} = \mu_y + \Lambda \mathbf{D} + \mathbf{H}. \quad (4)$$

From (4) we can see that $\mathbf{Y}|\mathbf{D} = \mathbf{d}$ is normally distributed with mean $\mu_y + \Lambda \mathbf{d}$ and covariance matrix Σ_y . Consequently, the joint density of $(\mathbf{Y}, \mathbf{D})^\top$ expressed as the product of the ones of $\mathbf{Y}|\mathbf{D}$ and \mathbf{D} , is given by

$$f(\mathbf{y}, \mathbf{d}) = 2^q \phi_q(\mathbf{y}|\mu_y + \Lambda \mathbf{d}, \Sigma_y) \phi_q(\mathbf{d}|\mathbf{0}_q, \mathbf{I}_q). \quad (5)$$

2.3 The joint linear-circular distribution

In this section we define the poly-cylindrical distribution starting from the augmented circular and linear marginals shown in equations (2) and (5). As in the previous sections, we indicate with p and q the dimensions of the vectors of circular and linear variables, respectively.

It is natural to introduce dependence between Θ and \mathbf{Y} by substituting the two normal pdfs of the augmented representation, i.e., $\phi_{2p}(\mathbf{w}|\mu_w, \Sigma_w)$ and $\phi_q(\mathbf{y}|\mu_y + \text{diag}(\lambda)\mathbf{d}, \Sigma_y)$, with a $2p+q$ normal pdf that has the two pdfs as marginals; after marginalization we obtain the density of $(\Theta, \mathbf{Y})^\top$. More precisely, we define the joint density of $(\Theta, \mathbf{R}, \mathbf{Y}, \mathbf{D})^\top$ as

$$f(\theta, \mathbf{r}, \mathbf{y}, \mathbf{d}) = 2^q \phi_{2p+q}((\mathbf{w}, \mathbf{y})^\top | \mu + (\mathbf{0}_{2p}, \text{diag}(\lambda)\mathbf{d})^\top, \Sigma) \phi_q(\mathbf{d}|\mathbf{0}_q, \mathbf{I}_q) \prod_{i=1}^p r_i, \quad (6)$$

with $\mu = (\mu_w, \mu_y)^\top$ and

$$\Sigma = \begin{pmatrix} \Sigma_w & \Sigma_{wy} \\ \Sigma_{wy}^\top & \Sigma_y \end{pmatrix}.$$

We then say that $(\Theta, \mathbf{Y})^\top$ is marginally distributed as a (p, q) -variate *joint projected normal and skew-normal* with parameters μ , Σ and λ , i.e., $(\Theta, \mathbf{Y})^\top \sim \mathcal{JPNS}_{p,q}(\mu, \Sigma, \lambda)$. Since $(\mathbf{W}, \mathbf{Y})^\top | \mathbf{d} \sim N_{2p+q}(\mu + (\mathbf{0}_{2p}, \text{diag}(\lambda)\mathbf{d})^\top, \Sigma)$, transformation of \mathbf{W} into Θ using (1) implies that $(\Theta, \mathbf{Y})^\top$ is \mathcal{JPNS} distributed; this last remark can be used to easily simulate random samples from the \mathcal{JPNS} .

Closure under marginalization of the \mathcal{PN} and the \mathcal{SSN} shows that any subset of $(\Theta, \mathbf{Y})^\top$ is still \mathcal{JPNS} distributed (see equation (6)) and, as limit cases, $\Theta \sim \mathcal{PN}_p(\mu_w, \Sigma_w)$ and $\mathbf{Y} \sim \mathcal{SSN}_q(\mu_y, \Sigma_y, \text{diag}(\lambda))$. The flexibility of the \mathcal{PN} and \mathcal{SSN} are then inherited by the marginal distributions of our proposal

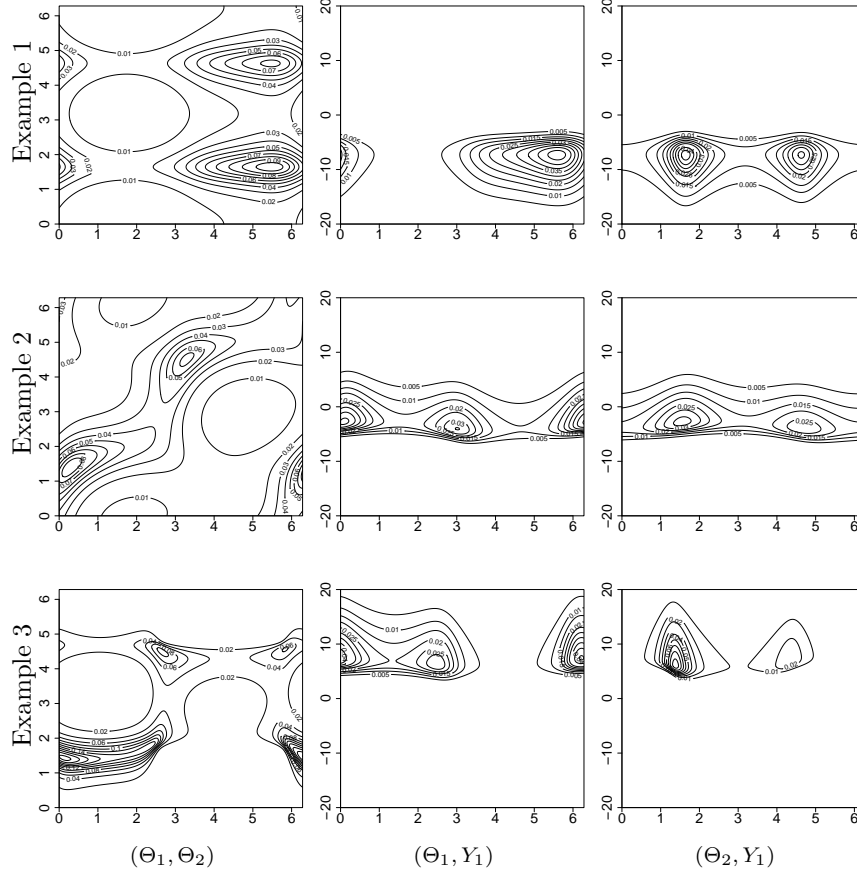


Figure 3: Bivariate marginal distributions of a $\mathcal{JPSN}_{2,1}(\boldsymbol{\mu}, \boldsymbol{\Sigma}, \boldsymbol{\lambda})$ under three sets of parameters (row) reported in Section 4.1. In the first column there are the marginal distributions of (Θ_1, Θ_2) , in the second those of (Θ_1, Y_1) and in the third the marginals of (Θ_2, Y_1) .

that allows also multivariate dependence between its components. Conditional densities are not standard, but from $(\mathbf{W}, \mathbf{Y})^\top | \mathbf{d} \sim N_{2p+q}(\boldsymbol{\mu} + (\mathbf{0}_{2p}, \text{diag}(\boldsymbol{\lambda})\mathbf{d})^\top, \boldsymbol{\Sigma})$ we can easily see that

$$\boldsymbol{\Theta} | \mathbf{y}, \mathbf{d} \sim \mathcal{PN}_p \left(\boldsymbol{\mu}_w + \boldsymbol{\Sigma}_{wy} \boldsymbol{\Sigma}_y^{-1} (\mathbf{y} - \boldsymbol{\mu}_y - \text{diag}(\boldsymbol{\lambda})\mathbf{d}), \boldsymbol{\Sigma}_w + \boldsymbol{\Sigma}_{wy} \boldsymbol{\Sigma}_y^{-1} \boldsymbol{\Sigma}_{wy}^\top \right)$$

and

$$\mathbf{Y} | \boldsymbol{\theta}, \mathbf{r} \sim \mathcal{SSN}_q \left(\boldsymbol{\mu}_y + \text{diag}(\boldsymbol{\lambda})\mathbf{d} + \boldsymbol{\Sigma}_{wy}^\top \boldsymbol{\Sigma}_w^{-1} (\mathbf{w} - \boldsymbol{\mu}_w), \boldsymbol{\Sigma}_y + \boldsymbol{\Sigma}_{wy}^\top \boldsymbol{\Sigma}_w^{-1} \boldsymbol{\Sigma}_{wy} \right).$$

\mathcal{JPSN} shapes are depicted in Figure 3.

Notice that $\Theta_i \perp \Theta_j$, where \perp indicates independence, iff $\mathbf{W}_i \perp \mathbf{W}_j$ and, by construction, matrix $\boldsymbol{\Sigma}_{wy}$ rules the circular-linear dependence since iff $\mathbf{W}_i \perp Y_j$ then $\Theta_i \perp Y_j$. Parameters $\boldsymbol{\mu}_y$ and $\boldsymbol{\Sigma}_y$ are easily interpretable since $E(\mathbf{Y}) = \boldsymbol{\mu}_y + \boldsymbol{\lambda}\sqrt{2/\pi}$, $\text{Var}(\mathbf{Y}) = \boldsymbol{\Sigma}_y + (1 - 2/\pi) \text{diag}(\boldsymbol{\lambda})\text{diag}(\boldsymbol{\lambda})$ and if $[\boldsymbol{\Sigma}_y]_{j,k} = 0$, where $[\boldsymbol{\Sigma}_y]_{j,k}$ indicates the element positioned in the j^{th} row and k^{th} column, then Y_j and Y_k are independent. $\boldsymbol{\lambda}$ controls the skewness of the linear component and Y_i is normally distributed if $\lambda_i = 0$. Parameters $\boldsymbol{\mu}_{w_i}$ and $\boldsymbol{\Sigma}_{w_i}$ determine the shape of the density of Θ_i , that is always \mathcal{PN} . It is not clear how changing one of the element of $\boldsymbol{\mu}_{w_i}$ or $\boldsymbol{\Sigma}_{w_i}$ affects the density, but special cases exist: a circular uniform distribution is obtained with $\boldsymbol{\mu}_{w_i} = \mathbf{0}_2$ and $\boldsymbol{\Sigma}_{w_i} = d\mathbf{I}_2$, $\boldsymbol{\mu}_{w_i} = \mathbf{0}_2$ produces

an antipodal density and $\mathcal{PN}(\boldsymbol{\mu}_{w_i}, d\mathbf{I}_2)$ is unimodal and symmetric. All the other statistics of the distribution that cannot be computed directly from the parameters, e.g., the circular mean, can be approximated with MC procedures.

3 Identifiability and Bayesian inference

Let \mathbf{C}_w be a $2p \times 2p$ diagonal matrix with $(2(i-1) + j) - th$ entry equal to $c_i > 0$, where $i = 1, \dots, p$ and $j = 1, 2$. Then, since

$$\Theta_i = \text{atan}^* \frac{W_{i2}}{W_{i1}} = \text{atan}^* \frac{c_i W_{i2}}{c_i W_{i1}}, \quad (7)$$

the two random vectors $\mathbf{W}_i \sim \mathcal{N}_2(\boldsymbol{\mu}_w, \boldsymbol{\Sigma}_w)$ and $\mathbf{C}_w \mathbf{W}_i \sim \mathcal{N}_{2p}(\mathbf{C}_w \boldsymbol{\mu}_w, \mathbf{C}_w \boldsymbol{\Sigma}_w \mathbf{C}_w)$ produce the same $\boldsymbol{\Theta}$, i.e., the c_i s cancel out in equation (7). It follows that $\{\boldsymbol{\mu}_w, \boldsymbol{\Sigma}_w\}$ and $\{\mathbf{C}_w \boldsymbol{\mu}_w, \mathbf{C}_w \boldsymbol{\Sigma}_w \mathbf{C}_w\}$ represent the same \mathcal{PN} density which is then not identifiable.

The \mathcal{JPSN} is based on the \mathcal{PN} , that is also its circular marginal distribution, and it has the same identification issue; for identifiability constraints on the parameters space are needed. Following and extending Wang and Gelfand (2013), we set to one the variance of each W_{i2} and from now on, to avoid confusion, we indicate $\{\boldsymbol{\mu}, \boldsymbol{\Sigma}, \mathbf{W}, \mathbf{R}\}$ as $\{\tilde{\boldsymbol{\mu}}, \tilde{\boldsymbol{\Sigma}}, \tilde{\mathbf{W}}, \tilde{\mathbf{R}}\}$ when such constraints are imposed; $\boldsymbol{\lambda}$, \mathbf{D} , $\boldsymbol{\mu}_y$ and $\boldsymbol{\Sigma}_y$ are always identified since they are related only to the linear component. Let

$$\mathbf{C} = \begin{pmatrix} \mathbf{C}_w & \mathbf{0}_{2p,q} \\ \mathbf{0}_{2p,q}^\top & \mathbf{I}_q \end{pmatrix},$$

where $\mathbf{0}_{2p,q}^\top$ is a $2p \times q$ zero matrix, then the sets $\{\tilde{\boldsymbol{\mu}}, \tilde{\boldsymbol{\Sigma}}, \boldsymbol{\lambda}\}$ and $\{\boldsymbol{\mu}, \boldsymbol{\Sigma}, \boldsymbol{\lambda}\}$ with

$$\begin{aligned} \boldsymbol{\mu} &= \mathbf{C} \tilde{\boldsymbol{\mu}}, \\ \boldsymbol{\Sigma} &= \mathbf{C} \tilde{\boldsymbol{\Sigma}} \mathbf{C}, \end{aligned}$$

produce the same \mathcal{JPSN} density and the following relation holds:

$$\begin{aligned} f(\boldsymbol{\theta}, \tilde{\mathbf{r}}, \mathbf{y}, \mathbf{d}) &= 2^q \phi_{2p+q}((\tilde{\mathbf{w}}, \mathbf{y})^\top | \tilde{\boldsymbol{\mu}} + (\mathbf{0}_{2p}, \text{diag}(\boldsymbol{\lambda}) \mathbf{d})^\top, \tilde{\boldsymbol{\Sigma}}) \phi_q(\mathbf{d} | \mathbf{0}_q, \mathbf{I}_q) \prod_{i=1}^p \tilde{r}_i = \\ &= 2^q \phi_{2p+q}(\mathbf{C}(\tilde{\mathbf{w}}, \mathbf{y})^\top | \mathbf{C} \tilde{\boldsymbol{\mu}} + (\mathbf{0}_{2p}, \text{diag}(\boldsymbol{\lambda}) \mathbf{d})^\top, \mathbf{C} \tilde{\boldsymbol{\Sigma}} \mathbf{C}) \phi_q(\mathbf{d} | \mathbf{0}_q, \mathbf{I}_q) \prod_{i=1}^p c_i \tilde{r}_i. \end{aligned} \quad (8)$$

Notice that there is a one-to-one relation between sets $\{\boldsymbol{\mu}, \boldsymbol{\Sigma}\}$ and $\{\tilde{\boldsymbol{\mu}}, \tilde{\boldsymbol{\Sigma}}, \mathbf{C}\}$ since $c_i = \sqrt{[\boldsymbol{\Sigma}]_{2i,2i}}$.

Due to the unavailability of MCMC algorithms for a constrained covariance matrix estimate, a computational problem arises and we show how to overcome it in the next section.

3.1 The MCMC algorithm

Suppose to have T observations drawn from a (p, q) -variate \mathcal{JPSN} , i.e., $(\boldsymbol{\Theta}_t, \mathbf{Y}_t)^\top \sim \mathcal{JPSN}_{p,q}(\tilde{\boldsymbol{\mu}}, \tilde{\boldsymbol{\Sigma}}, \boldsymbol{\lambda})$ with $t = 1, \dots, T$. As the \mathcal{JPSN} does not have a closed form density, we introduce $\tilde{\mathbf{R}}_t = \{\tilde{R}_{ti}\}_{i=1}^p$ and \mathbf{D}_t as latent variables and letting $g_1(\tilde{\boldsymbol{\mu}}, \tilde{\boldsymbol{\Sigma}} | \boldsymbol{\lambda}) g_2(\boldsymbol{\lambda})$ be the prior distribution, we want to evaluate the posterior of $\{\{\tilde{\mathbf{R}}_t\}_{t=1}^T, \{\mathbf{D}_t\}_{t=1}^T, \tilde{\boldsymbol{\mu}}, \tilde{\boldsymbol{\Sigma}}, \boldsymbol{\lambda}\}$ given by

$$\frac{\prod_{t=1}^T 2^q \phi_{2p+q}((\tilde{\mathbf{w}}_t, \mathbf{y}_t)^\top | \tilde{\boldsymbol{\mu}} + (\mathbf{0}_{2p}, \text{diag}(\boldsymbol{\lambda}) \mathbf{d}_t)^\top, \tilde{\boldsymbol{\Sigma}}) \phi_q(\mathbf{d}_t | \mathbf{0}_q, \mathbf{I}_q) \prod_{i=1}^p \tilde{r}_{ti} g_1(\tilde{\boldsymbol{\mu}}, \tilde{\boldsymbol{\Sigma}} | \boldsymbol{\lambda}) g_2(\boldsymbol{\lambda})}{Z(\{\boldsymbol{\theta}_t, \mathbf{y}_t\}_{t=1}^T)}, \quad (9)$$

where $Z(\{\boldsymbol{\theta}_t, \mathbf{y}_t\}_{t=1}^T)$ is the normalization constant. Some difficulties arise in the definition of $g_1(\cdot)$ since its domain must contain the space of constrained nnd matrices and, to the best of our knowledge, no priors with such domain are available.

Our proposed MCMC algorithm starts defining a prior $f(\boldsymbol{\mu}, \boldsymbol{\Sigma}|\boldsymbol{\lambda})$ over $\{\boldsymbol{\mu}, \boldsymbol{\Sigma}\}$. We indicate with $f^*(\mathbf{C}, \tilde{\boldsymbol{\mu}}, \tilde{\boldsymbol{\Sigma}}|\boldsymbol{\lambda})$ the distribution over $\{\mathbf{C}, \tilde{\boldsymbol{\mu}}, \tilde{\boldsymbol{\Sigma}}\}$ induced by $f(\boldsymbol{\mu}, \boldsymbol{\Sigma}|\boldsymbol{\lambda})$ and we define $g_1(\tilde{\boldsymbol{\mu}}, \tilde{\boldsymbol{\Sigma}}|\boldsymbol{\lambda})$ as

$$g_1(\tilde{\boldsymbol{\mu}}, \tilde{\boldsymbol{\Sigma}}|\boldsymbol{\lambda}) = \int_{\mathbb{R}^+} \dots \int_{\mathbb{R}^+} f^*(\mathbf{C}, \tilde{\boldsymbol{\mu}}, \tilde{\boldsymbol{\Sigma}}|\boldsymbol{\lambda}) dc_1 \dots dc_p. \quad (10)$$

Then, using (8) and (10) we can write (9) as

$$\begin{aligned} \int_{\mathbb{R}^+} \dots \int_{\mathbb{R}^+} \prod_{t=1}^T 2^q \phi_{2p+q}(\mathbf{C}(\tilde{\mathbf{w}}_t, \mathbf{y}_t)^\top | \mathbf{C}\tilde{\boldsymbol{\mu}} + (\mathbf{0}_{2p}, \text{diag}(\boldsymbol{\lambda})\mathbf{d})^\top, \mathbf{C}\tilde{\boldsymbol{\Sigma}}\mathbf{C}) \times \\ \frac{\phi_q(\mathbf{d}_t | \mathbf{0}_q, \mathbf{I}_q) \prod_{i=1}^p c_i \tilde{r}_{ti} f^*(\mathbf{C}, \tilde{\boldsymbol{\mu}}, \tilde{\boldsymbol{\Sigma}}|\boldsymbol{\lambda}) g_2(\boldsymbol{\lambda})}{Z(\{\boldsymbol{\theta}_t, \mathbf{y}_t\}_{t=1}^T)} dc_1 \dots dc_p, \end{aligned} \quad (11)$$

and if we transform $\{\mathbf{C}, \{\tilde{\mathbf{R}}_t\}_{t=1}^T, \tilde{\boldsymbol{\mu}}, \tilde{\boldsymbol{\Sigma}}\}$ into $\{\{\mathbf{R}_t\}_{t=1}^T, \boldsymbol{\mu}, \boldsymbol{\Sigma}\}$, the integrand of equation (11) becomes

$$\frac{\prod_{t=1}^T \phi_{2p+q}((\mathbf{w}_t, \mathbf{y}_t)^\top | \boldsymbol{\mu} + (\mathbf{0}_{2p}, \text{diag}(\boldsymbol{\lambda})\mathbf{d}_t)^\top, \boldsymbol{\Sigma}) \phi_q(\mathbf{d}_t | \mathbf{0}_q, \mathbf{I}_q) \prod_{i=1}^p r_{ti} f(\boldsymbol{\mu}, \boldsymbol{\Sigma}|\boldsymbol{\lambda}) g_2(\boldsymbol{\lambda})}{Z(\{\boldsymbol{\theta}_t, \mathbf{y}_t\}_{t=1}^T)}. \quad (12)$$

Then, relying on standard MC integration rules (see for example Brooks et al., 2011; Robert and Casella, 2005), a set of B draws from (9) is obtained by taking B samples of $\{\{\mathbf{R}_t\}_{t=1}^T, \{\mathbf{D}_t\}_{t=1}^T, \boldsymbol{\mu}, \boldsymbol{\Sigma}, \boldsymbol{\lambda}\}$ from (12) and transforming them to $\{\{\tilde{\mathbf{R}}_t\}_{t=1}^T, \tilde{\boldsymbol{\mu}}, \tilde{\boldsymbol{\Sigma}}, \boldsymbol{\lambda}\}$.

In a schematic way our proposal is

- to define a prior over $\{\boldsymbol{\mu}, \boldsymbol{\Sigma}, \boldsymbol{\lambda}\}$ that induces a prior $g_1(\cdot)$ (see equation (10));
- to obtain a set of samples of $\{\{\mathbf{R}_t\}_{t=1}^T, \{\mathbf{D}_t\}_{t=1}^T, \boldsymbol{\mu}, \boldsymbol{\Sigma}, \boldsymbol{\lambda}\}$ from distribution (12);
- to transform the posterior samples of $\{\{\mathbf{R}_t\}_{t=1}^T, \boldsymbol{\mu}, \boldsymbol{\Sigma}\}$ into $\{\{\tilde{\mathbf{R}}_t\}_{t=1}^T, \tilde{\boldsymbol{\mu}}, \tilde{\boldsymbol{\Sigma}}\}$ after the model fitting.

The resulting posterior samples are from the distribution of interest (equation (9)). The proposed MCMC algorithm can be used with the $\mathcal{JP}\mathcal{SN}$, the univariate projected normal ($q = 0$ and $p = 1$), the multivariate projected normal ($q = 0$) and also with the proposal of (Hernandez-Stumpfhauser et al., 2016), i.e., a distribution defined over the K -dimensional sphere, since all of them share the same identification problem.

There are no restrictions on the choice of $g_1(\cdot)$ and $g_2(\cdot)$ but, as shown in Appendix B, if ease of implementation and conjugate priors are required, a normal inverse-Wishart (\mathcal{NIW}) can be used for $\{\boldsymbol{\mu}, \boldsymbol{\Sigma}\}$ and a normal for $\boldsymbol{\lambda}$; these are the ones we use in the examples of Section 4. Regardless of the priors chosen, the updates of \mathbf{D}_t and R_{ti} can be done using Gibbs steps.

4 Examples

4.1 Synthetic data

The aim of these simulated examples is to prove that the proposed MCMC algorithm is able to retrieve the parameters used to simulate the data and to solve the identification problem. We simulate 3 datasets with $p = 2$, $q = 1$, i.e., two circular variables and 1 linear, $T = 1000$ and parameters

$$\tilde{\boldsymbol{\mu}}_1 = \begin{bmatrix} 0.5 \\ -1.0 \\ -0.1 \\ 0.1 \\ -5.0 \end{bmatrix}, \quad \tilde{\boldsymbol{\mu}}_2 = \begin{bmatrix} 0.2 \\ 0.2 \\ 0.0 \\ 0.1 \\ -5.0 \end{bmatrix}, \quad \tilde{\boldsymbol{\mu}}_3 = \begin{bmatrix} 0.5 \\ 0.5 \\ 0.0 \\ 0.5 \\ 5.0 \end{bmatrix},$$

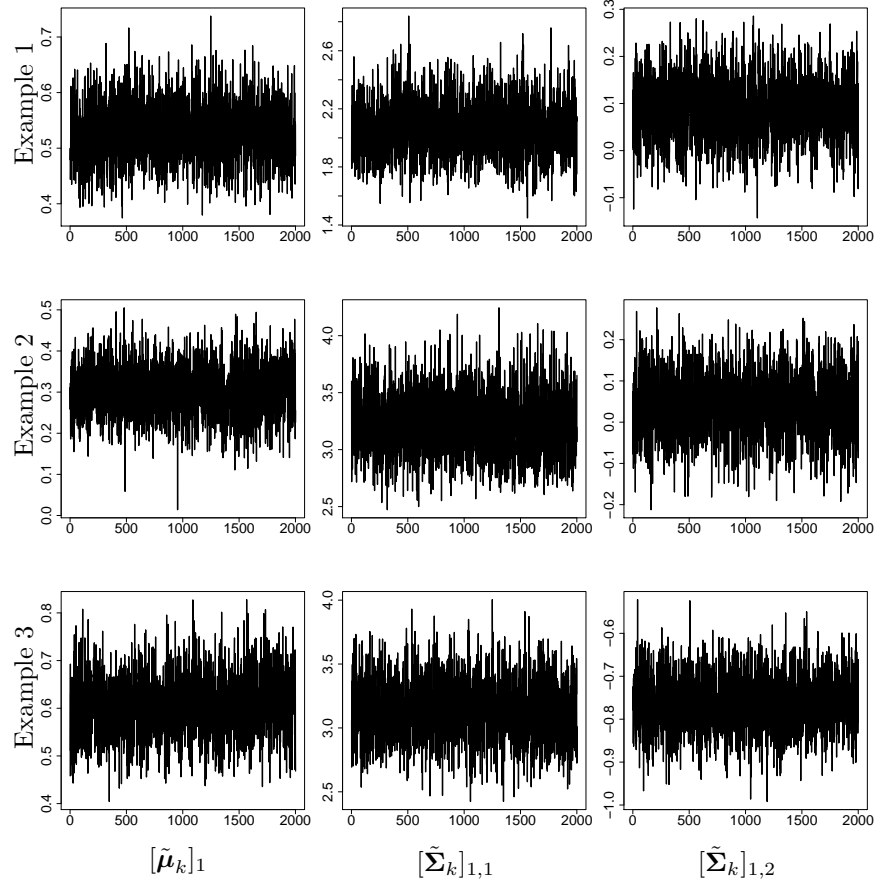


Figure 4: Simulated examples - trace plots of parameters $[\tilde{\mu}_k]_1$, $[\tilde{\Sigma}_k]_{1,1}$ and $[\tilde{\Sigma}_k]_{1,2}$ (columns) in the three examples (rows)

	Example		
	k=1	k=2	k=3
$[\hat{\mu}_k]_1$	0.529	0.301	0.608
CI	(0.428 0.638)	(0.179 0.427)	(0.480 0.738)
$[\hat{\mu}_k]_2$	-0.943	0.207	0.5
CI	(-1.029 -0.858)	(0.137 0.280)	(0.428 0.576)
$[\hat{\mu}_k]_3$	-0.112	-0.02	0.007
CI	(-0.145 -0.080)	(-0.068 0.029)	(-0.023 0.036)
$[\hat{\mu}_k]_4$	0.095	0.111	0.503
CI	(0.020 0.163)	(0.041 0.178)	(0.429 0.576)
$[\hat{\mu}_k]_5$	-5.095	-4.765	4.705
CI	(-5.415 -4.780)	(-4.925 -4.596)	(4.489 5.105)
$\hat{\lambda}_k$	-4.941	4.872	6.237
CI	(-5.320 -4.561)	(4.630 5.135)	(5.920 6.556)

Table 1: Simulated examples - posterior mean estimates ($\hat{\cdot}$) and 95% credible intervals (CI) of $\tilde{\mu}_k$ and λ_k .

	j=1	j=2	j=3	j=4	j=5
$\hat{\tilde{\Sigma}}_1]_{1,j}$	2.062	0.085	-0.031	0.011	-0.001
CI	(1.726 2.462)	(-0.040 0.214)	(-0.083 0.021)	(-0.098 0.121)	(-0.287 0.278)
$\hat{\tilde{\Sigma}}_1]_{2,j}$.	1	-0.008	-0.009	0.149
CI	(. .)	(1 1)	(-0.046 0.028)	(-0.094 0.075)	(-0.060 0.368)
$\hat{\tilde{\Sigma}}_1]_{3,j}$.	.	0.201	0.002	0.007
CI	(. .)	(. .)	(0.168 0.237)	(-0.039 0.041)	(-0.079 0.097)
$\hat{\tilde{\Sigma}}_1]_{4,j}$.	.	.	1	0.047
CI	(. .)	(. .)	(. .)	(1 1)	(-0.144 0.248)
$\hat{\tilde{\Sigma}}_1]_{5,j}$	2.151
CI	(. .)	(. .)	(. .)	(. .)	(1.532 2.908)
$\hat{\tilde{\Sigma}}_2]_{1,j}$	3.23	0.04	0.581	0.862	0.882
CI	(2.719 3.793)	(-0.112 0.191)	(0.467 0.713)	(0.722 1.015)	(0.619 1.151)
$\hat{\tilde{\Sigma}}_2]_{2,j}$.	1	-0.293	0.429	0.419
CI	(. .)	(1 1)	(-0.354 -0.235)	(0.361 0.492)	(0.284 0.557)
$\hat{\tilde{\Sigma}}_2]_{3,j}$.	.	0.521	0.034	-0.223
CI	(. .)	(. .)	(0.438 0.617)	(-0.024 0.095)	(-0.333 -0.120)
$\hat{\tilde{\Sigma}}_2]_{4,j}$.	.	.	1	0.496
CI	(. .)	(. .)	(. .)	(1 1)	(0.354 0.645)
$\hat{\tilde{\Sigma}}_2]_{5,j}$	1.001
CI	(. .)	(. .)	(. .)	(. .)	(0.737 1.316)
$\hat{\tilde{\Sigma}}_3]_{1,j}$	3.129	-0.762	0.38	0.623	0.834
CI	(2.684 3.620)	(-0.889 -0.633)	(0.309 0.455)	(0.469 0.775)	(0.566 1.132)
$\hat{\tilde{\Sigma}}_3]_{2,j}$.	1	0.207	0.389	-0.176
CI	(. .)	(1 1)	(0.177 0.238)	(0.319 0.458)	(-0.325 -0.021)
$\hat{\tilde{\Sigma}}_3]_{3,j}$.	.	0.189	0.223	0.17
CI	(. .)	(. .)	(0.164 0.216)	(0.193 0.255)	(0.108 0.240)
$\hat{\tilde{\Sigma}}_3]_{4,j}$.	.	.	1	-0.337
CI	(. .)	(. .)	(. .)	(1 1)	(-0.493 -0.188)
$\hat{\tilde{\Sigma}}_3]_{5,j}$	0.875
CI	(. .)	(. .)	(. .)	(. .)	(0.620 1.165)

Table 2: Simulated examples - posterior mean estimates ($\hat{\cdot}$) and 95% credible intervals (CI) of $\tilde{\Sigma}_k$.

$\lambda_1 = -5, \lambda_2 = 5, \lambda_3 = 6,$

$$\tilde{\Sigma}_1 = \begin{bmatrix} 2 & 0 & 0.0 & 0 & 0 \\ 0 & 1 & 0.0 & 0 & 0 \\ 0 & 0 & 0.2 & 0 & 0 \\ 0 & 0 & 0.0 & 1 & 0 \\ 0 & 0 & 0.0 & 0 & 2 \end{bmatrix}, \quad \tilde{\Sigma}_2 = \begin{bmatrix} 3.000 & 0.000 & 0.551 & 0.779 & 0.857 \\ 0.000 & 1.000 & -0.318 & 0.450 & 0.495 \\ 0.551 & -0.318 & 0.500 & 0.000 & -0.318 \\ 0.779 & 0.450 & 0.000 & 1.000 & 0.450 \\ 0.857 & 0.495 & -0.318 & 0.450 & 1.000 \end{bmatrix},$$

$$\tilde{\Sigma}_3 = \begin{bmatrix} 3.000 & -0.783 & 0.377 & 0.684 & 0.781 \\ -0.783 & 1.000 & 0.214 & 0.335 & -0.092 \\ 0.377 & 0.214 & 0.200 & 0.231 & 0.209 \\ 0.684 & 0.335 & 0.231 & 1.000 & -0.382 \\ 0.781 & -0.092 & 0.209 & -0.382 & 1.000 \end{bmatrix}.$$

The marginal bivariate densities are plotted in Figure 3. We chose the parameters so to have independent (first example) and dependent variables (second and third), highly skew linear densities and, at least, one bimodal circular marginal for each example.

In the three examples inference is carried out considering 40000 iterations, burnin 30000, thin 5 and by taking 2000 posterior samples. As prior distributions we choose $\boldsymbol{\mu}_k, \boldsymbol{\Sigma}_k \sim \mathcal{N}\mathcal{IW}(\mathbf{0}_5, 0.001, 15, \mathbf{I}_5)$ and $\lambda_k \sim \mathcal{N}_1(0, 100)$, that are standard weak informative priors. From Tables 1 and 2 we see that, with the exception of $[\hat{\boldsymbol{\mu}}_2]_5$, all true values are inside the associated 95% credible intervals (CIs), proving that our algorithm is able to estimate the \mathcal{JPSN} parameters. To further corroborate the validity of the proposed MCMC scheme in solving the identification problem, in Figure 4 we show, as examples, the trace plots of parameters $[\hat{\boldsymbol{\mu}}_k]_1, [\hat{\boldsymbol{\Sigma}}_k]_{1,1}$ and $[\hat{\boldsymbol{\Sigma}}_k]_{1,2}$. These chains have reached their stationary distributions (we also checked it by using the R package `coda` (Plummer et al., 2006)) with weak informative priors; this shows that the identification problem is no more relevant.

4.2 Zebras movements example

In this section we estimate the \mathcal{JPSN} parameters on an animal movement dataset taken from the movebank repository (www.movebank.org). Our aim is to show that the \mathcal{JPSN} can give information on the dependence of poly-cylindrical observations. Seven zebras are jointly observed in Botswana (Africa) between the Okavango Delta and the Makgadikgadi Pans, and their hourly positions are recorded with GPS devices during the years 2007-2009 (Bartlam-Brooks et al., 2013). In the observational period the zebras migrate from the dry season habitat, that is the Okavango Delta, to the rainy season habitat, that is the Makgadikgadi Pans. We select data from 4 zebras, observed between the 18 of November 2008 and the 18 of February 2009, when they have ended the migration. For each animal we compute the turning-angles and logarithm of step-lengths, having then poly-cylindrical observations composed of four circular and four linear variables. It is out of the scope of this work to introduce complex models based on the \mathcal{JPSN} , that are left to future developments, and we assume that observations are independent and identical distributed. For this reason, to mitigate temporal dependence we use data five hours apart, having then 442 observations for parameters estimate. Using the Pearson's coefficient and the circular-circular correlation of Jammalamadaka and Sarma (1988), i.e.,

$$\rho_{(\Theta_i, \Theta_{i'})} = \frac{E(\sin(\Theta_i - \Theta_i^*) \sin(\Theta_{i'} - \Theta_{i'}^*))}{\sqrt{E(\sin^2(\Theta_i - \Theta_i^*))E(\sin^2(\Theta_{i'} - \Theta_{i'}^*))}} \in [-1, 1], \quad (13)$$

where Θ_i^* and $\Theta_{i'}^*$ are two circular variables distributed, respectively, as Θ_i and $\Theta_{i'}$, for the subset of data used all the autocorrelations have values lower than 0.05. The histograms of the data can be seen in Figure 5.

The MCMC algorithm is implemented using the same number of iterations, thin and burnin used in the previous section while $\{\boldsymbol{\mu}, \boldsymbol{\Sigma}\} \sim \mathcal{N}\mathcal{IW}(\mathbf{0}_{12}, 0.001, 15, \mathbf{I}_{12})$ and $\boldsymbol{\lambda} \sim \mathcal{N}_4(0, 100\mathbf{I}_4)$. In Figure 5 and 6 we depicted, respectively, the marginal posterior \mathcal{JPSN} densities and the dependence matrix. The

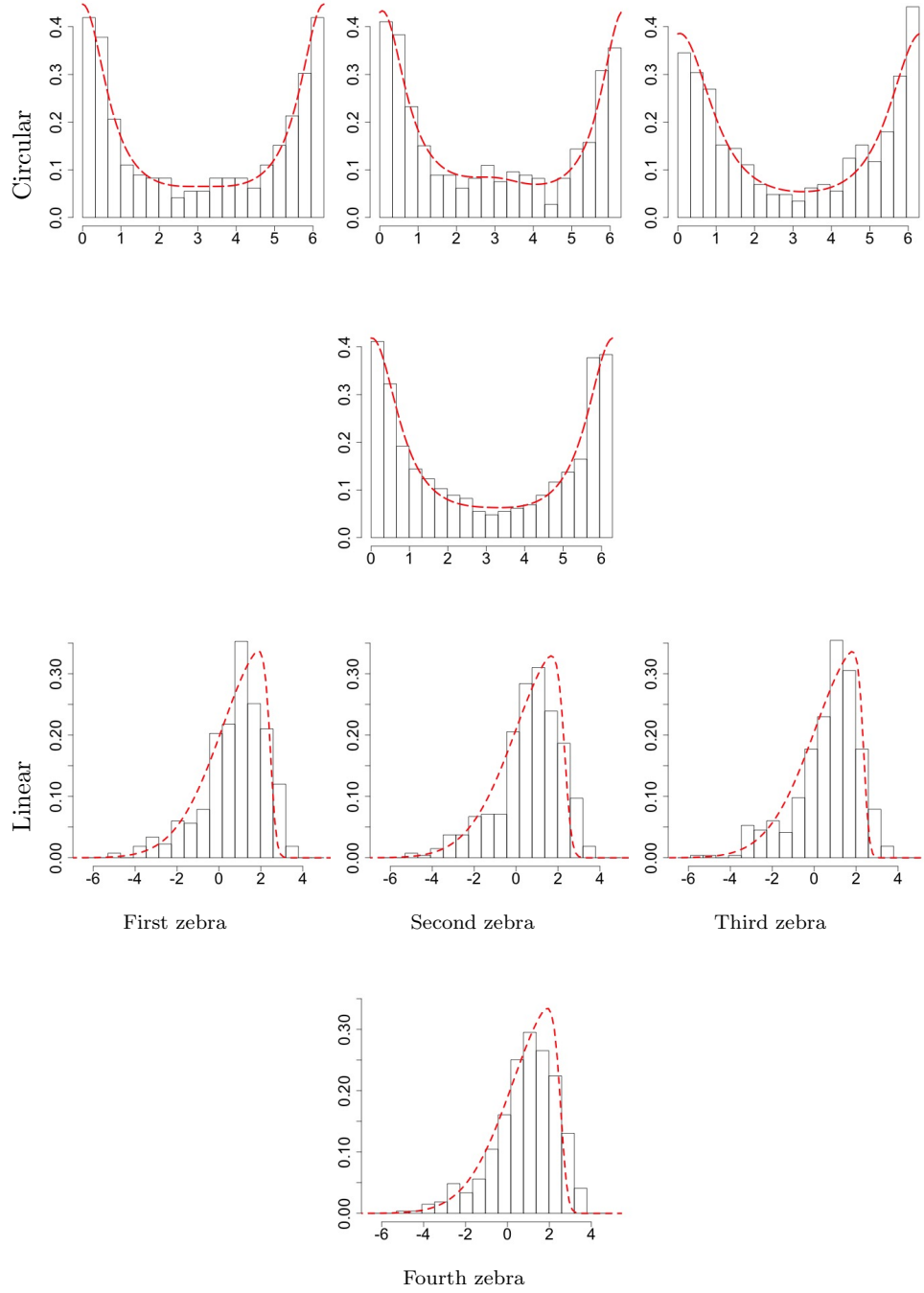


Figure 5: Zebras movement example - histograms of the observed data and posterior marginal densities of turning-angles (first row) and the logarithm of step-lengths (second row).

latter shows the MC estimates of the posterior mean circular-circular correlation of Jammalamadaka

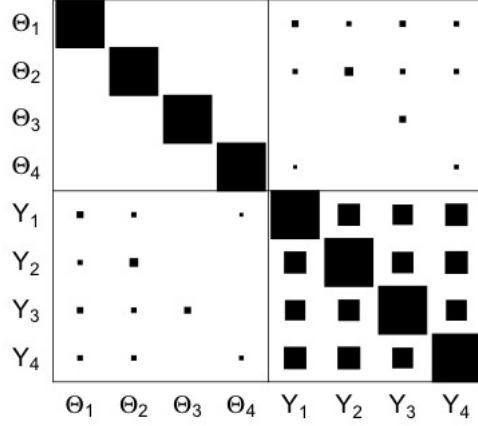


Figure 6: Zebras movement example - dependence matrix computed using equations (13) (circular-circular), (14) (circular-linear) and the Pearson’s correlation coefficient (linear-linear). The size of the square is proportional to the posterior mean value. All values are positive.

and Sarma (1988), the circular-linear dependence of Mardia (1976), i.e.,

$$\rho_{(\Theta_i, Y_j)}^2 = \frac{\text{Cor}(\cos \Theta_i, Y_j)^2 + \text{Cor}(\sin \Theta_i, Y_j)^2}{1 - \text{Cor}(\cos \Theta_i, \sin \Theta_i)} + \frac{-2\text{Cor}(\cos \Theta_i, Y_j)\text{Cor}(\sin \Theta_i, Y_j)\text{Cor}(\cos \Theta_i, \sin \Theta_i)}{1 - \text{Cor}(\cos \Theta_i, \sin \Theta_i)} \in [0, 1], \quad (14)$$

and linear-linear correlation, evaluated with the Pearson’s coefficient. A circular-circular and linear-linear correlation is plotted only if the associated CI does not contain zero while since the CI of $\rho^2(\Theta_i, Y_j)$ has 0 probability to contain the 0, we plot the value of $\rho^2(\Theta_i, Y_j)$ using a different rationality. More precisely, since $\mathbf{W}_i \perp Y_j$ iff $\Theta_i \perp Y_j$, in Figure 6 we plot the posterior mean value of $\rho^2(\Theta_i, Y_j)$ only if at least one of the CIs of Σ_{wy} that measure the correlation between \mathbf{W}_i and Y_j does not contain the zero. From Figure 5 we appreciate that the \mathcal{JPSN} is able to fit satisfactorily the data and to find significant circular-linear and linear-linear correlations (Figure 6).

4.3 Comparison with cylindrical distributions

With this section we want to demonstrate that ignoring multivariate dependence leads to loss of predictive ability. Then we compare our proposal with the cylindrical distribution of Abe-Ley (Abe and Ley, 2017) and a cylindrical version of the \mathcal{JPSN} , i.e., for both we assume dependence between the variables belonging to the same animal and independence between zebras. Since the \mathcal{JPSN} is not available in closed form, a comparison based on informational criteria, such as AIC or BIC, is not possible. We decide to make the comparison in terms of predictive ability measured used the CRPS, that is a proper scoring rule defined for both circular (Grimet et al., 2006) and linear (Gneiting and Raftery, 2007) variables that measure the distance between cumulative distribution functions (Matheson and Winkler, 1976); lower values are then preferable. The Abe-Ley distribution is defined only for a positive linear variable and then, to make a fair comparison, we use the distribution that

arises by taking the logarithm of its linear component:

$$f(\theta_i, y_j) = \frac{\alpha^{AL}(\beta^{AL})^{\alpha^{AL}}}{2\pi \cosh \kappa^{AL}} (1 + \lambda^{AL} \sin(\theta_i - \mu^{AL})) e^{y_j(\alpha^{AL}-1)} e^{-(\beta^{AL} e^{y_j})^{\alpha^{AL}} (1 - \tanh \kappa^{AL} \cos(\theta_i - \mu^{AL}))} e^{y_j}.$$

$\alpha^{AL} \in \mathbb{R}^+$ and $\beta^{AL} \in \mathbb{R}^+$ are linear scale and shape parameters, $\mu^{AL} \in [0, 2\pi)$ and $\lambda^{AL} \in [-1, 1]$ endorse the role of circular location and skewness parameters and $\kappa^{AL} \in \mathbb{R}^+$ plays the role of circular concentration and circular-linear dependence parameter. For the Abe-Ley parameters we use standard weak informative priors, i.e., an inverse gamma with parameters (1,1) for α^{AL} , β^{AL} and κ^{AL} while uniform distributions on the respective domains are used for μ^{AL} and λ^{AL} . Under the cylindrical \mathcal{JPSN} , a $\mathcal{N}_1(0, 100)$ is used for the skewness parameters and a $\mathcal{NTW}(\mathbf{0}_3, 0.001, 6, \mathbf{I}_3)$ for the others that are the marginal priors deriving from the ones of the poly-cylindrical \mathcal{JPSN} .

We select 10% of the circular and linear observations to be set aside and not used to estimate the posterior distributions. We predict their values based on the posterior samples and we measure how the models perform in term of posterior estimates. Then, let $\mathcal{C}_i \subset \{1, 2, \dots, T\}$ and $\mathcal{L}_j \subset \{1, \dots, T\}$ be sets of indices, where $t \in \mathcal{C}_i$ if θ_{ti} is missing and $t \in \mathcal{L}_j$ if y_{tj} is missing, and let θ_{ti}^b , $t \in \mathcal{C}_i$, and y_{tj}^b , $t \in \mathcal{L}_j$, be, respectively, the b^{th} posterior sample of θ_{ti} and y_{tj} . An MC approximation of the CRPS for circular variables based on B posterior samples is computed as

$$CRPSc_i \approx \frac{1}{B} \sum_{b=1}^B d(\theta_{ti}, \theta_{ti}^b) - \frac{1}{2B^2} \sum_{b=1}^B \sum_{b'=1}^B d(\theta_{ti}^b, \theta_{ti}^{b'}), \quad t \in \mathcal{C}_i,$$

where $d(\cdot, \cdot)$ is the angular distance, while the CRPS for linear variable is approximated by

$$CRPSl_j \approx \frac{1}{B} \sum_{b=1}^B |y_{tj} - y_{tj}^b| - \frac{1}{2B^2} \sum_{b=1}^B \sum_{b'=1}^B |y_{tj}^b - y_{tj}^{b'}|, \quad t \in \mathcal{L}_j.$$

We then compute the overall mean CRPSs for the sets of circular and linear variables and we use these indices to measure the goodness-of-fit.

Circular and linear CRPSs have values 0.383 and 0.693 for the \mathcal{JPSN} , 0.385 and 0.762 for the cylindrical \mathcal{JPSN} , and 0.412 and 0.753 for the Abe-Ley density, showing that the \mathcal{JPSN} performs better and, moreover, it is also able to give a measure of dependence between all the circular and linear components (Figure 6) that is not possible with cylindrical distributions.

5 Concluding remarks

In this work we introduced a poly-cylindrical distribution. The proposal is highly flexible, it is closed under marginalization and it allows to have dependent components, bimodal marginal circular distributions and asymmetric linear ones. We showed how the MCMC algorithm, used to obtain posterior samples, can be easily implemented using only Gibbs steps. The proposal suffers from an identification problem and we showed how to overcome it with a post-processing of posterior samples that can also be used with the \mathcal{PN} distribution. With the aim to prove the validity of our sampling scheme, the algorithm was applied to simulated examples. Then the proposed distribution was used to model a real data taken from the movebank data repository. The predictive ability of our proposal was compared with the ones of cylindrical distributions, showing that the \mathcal{JPSN} performs better.

Future work will lead us to use the \mathcal{JPSN} as emission distribution in an hidden Markov model and to incorporate covariates to model mean and covariance of the circular-linear observations.

Acknowledgement

The author wishes to thank Antonello Maruotti, Giovanna Jona Lasinio and Alessio Pollice for assistance and comments that greatly improved the manuscript.

This work is partially developed under the PRIN2015 supported-project Environmental processes and human activities: capturing their interactions via statistical methods (EPHASTAT) funded by MIUR (Italian Ministry of Education, University and Scientific Research).

References

References

- Abe, T., Ley, C., 2017. A tractable, parsimonious and flexible model for cylindrical data, with applications. *Econometrics and Statistics* 4, 91 – 104.
- Anderson-Cook, C., 1997. An extension to modeling cylindrical variables. *Statistics and Probability Letters* 35, 215 – 223.
- Arellano-Valle, R., Bolfarine, H., Lachos, V., 2007. Bayesian inference for skew-normal linear mixed models. *Journal of Applied Statistics* 34, 663–682. doi:10.1080/02664760701236905.
- Azzalini, A., 1985. A class of distributions which includes the normal ones. *Scandinavian Journal of Statistics* 12, 171–178.
- Azzalini, A., Dalla Valle, A., 1996. The multivariate skew-normal distribution. *Biometrika* 83, 715–726. doi:10.1093/biomet/83.4.715.
- Bartlam-Brooks, H.L.A., Beck, P.S.A., Bohrer, G., Harris, S., 2013. In search of greener pastures: Using satellite images to predict the effects of environmental change on zebra migration. *Journal of Geophysical Research: Biogeosciences* 118, 1427–1437. doi:10.1002/jgrg.20096.
- Brooks, S., Gelman, A., Jones, G., Meng, X., 2011. *Handbook of Markov Chain Monte Carlo*. Chapman & Hall/CRC Handbooks of Modern Statistical Methods, CRC Press.
- Bulla, J., Lagona, F., Maruotti, A., Picone, M., 2012. A multivariate hidden Markov model for the identification of sea regimes from incomplete skewed and circular time series. *Journal of Agricultural, Biological, and Environmental Statistics* 17, 544–567. doi:10.1007/s13253-012-0110-1.
- D’Elia, A., 2001. A statistical model for orientation mechanism. *Statistical Methods and Applications* 10, 157–174. doi:10.1007/BF02511646.
- Gatto, R., Jammalamadaka, S.R., 2007. The generalized von mises distribution. *Statistical Methodology* 4, 341 – 353. doi:http://dx.doi.org/10.1016/j.stamet.2006.11.003.
- Gneiting, T., Raftery, A.E., 2007. Strictly proper scoring rules, prediction, and estimation. *Journal of the American Statistical Association* 102, 359–378.
- Grimit, E.P., Gneiting, T., Berrocal, V.J., Johnson, N.A., 2006. The continuous ranked probability score for circular variables and its application to mesoscale forecast ensemble verification. *Quarterly Journal of the Royal Meteorological Society* 132, 2925–2942. doi:10.1256/qj.05.235.
- Gupta, A.K., González-Farías, G., Dominguez-Molina, J., 2004. A multivariate skew normal distribution. *Journal of Multivariate Analysis* 89, 181 – 190. doi:http://dx.doi.org/10.1016/S0047-259X(03)00131-3.
- Hernandez-Stumpfhauser, D., Breidt, F.J., van der Woerd, M.J., 2016. The general projected normal distribution of arbitrary dimension: modeling and Bayesian inference. *Bayesian Analysis* doi:10.1214/15-BA989.

- Jammalamadaka, S., Sarma, Y., 1988. A correlation coefficient for angular variables. *Statistical Theory and Data Analysis II* , 349–364.
- Jammalamadaka, S.R., SenGupta, A., 2001. *Topics in Circular Statistics*. World Scientific, Singapore.
- Johnson, R.A., Wehrly, T.E., 1978. Some angular-linear distributions and related regression models. *Journal of the American Statistical Association* 73, 602–606.
- Jones, M.C., Pewsey, A., 2009. Sinh-arcsinh distributions. *Biometrika* 96, 761–780.
- Jonsen, I.D., Flemming, J.M., Myers, R.A., 2005. Robust state-space modeling of animal movement data. *Ecology* 86, 2874–2880.
- Lagona, F., Picone, M., 2011. A latent-class model for clustering incomplete linear and circular data in marine studies. *Journal of Data Science* 9.
- Mardia, K.V., 1976. Linear-circular correlation coefficients and rhythmometry. *Biometrika* 63.
- Mardia, K.V., Jupp, P.E., 1999. *Directional Statistics*. John Wiley and Sons, Chichester.
- Mardia, K.V., Sutton, T.W., 1978. A model for cylindrical variables with applications. *Journal of the Royal Statistical Society. Series B (Methodological)* 40, 229–233.
- Maruotti, A., Punzo, A., Mastrantonio, G., Lagona, F., 2015. A time-dependent extension of the projected normal regression model for longitudinal circular data based on a hidden Markov heterogeneity structure. *Stochastic Environmental Research and Risk Assessment* To appear.
- Mastrantonio, G., Calise, G., 2016. Hidden Markov model for discrete circular-linear wind data time series. *Journal of Statistical Computation and Simulation* To appear. doi:10.1080/00949655.2016.1142544.
- Mastrantonio, G., Jona Lasinio, G., Gelfand, A.E., 2015a. Spatio-temporal circular models with non-separable covariance structure. *TEST* To appear. doi:10.1007/s11749-015-0458-y.
- Mastrantonio, G., Jona Lasinio, G., Maruotti, A., Calise, G., 2017. Invariance properties and statistical inference for circular data. *Statistica Sinica* To appear.
- Mastrantonio, G., Maruotti, A., Jona Lasinio, G., 2015b. Bayesian hidden Markov modelling using circular-linear general projected normal distribution. *Environmetrics* 26, 145–158.
- Matheson, J.E., Winkler, R.L., 1976. Scoring rules for continuous probability distributions. *Management Science* 22, 1087–1096.
- Morales, J.M., Haydon, D.T., Frair, J., Holsinger, K.E., Fryxell, J.M., 2004. Extracting more out of relocation data: building movement models as mixtures of random walks. *Ecology* 85, 2436–2445.
- Morales, J.M., Moorcroft, P.R., Matthiopoulos, J., Frair, J.L., Kie, J.G., Powell, R.A., Merrill, E.H., Haydon, D.T., 2010. Building the bridge between animal movement and population dynamics. *Philosophical Transactions of the Royal Society B: Biological Sciences* 365, 2289–2301. doi:10.1098/rstb.2010.0082.
- Olmos, N.M., Varela, H., Gómez, H.W., Bolfarine, H., 2012. An extension of the half-normal distribution. *Statistical Papers* 53, 875–886. doi:10.1007/s00362-011-0391-4.
- Patterson, T., Thomas, L., Wilcox, C., Ovaskainen, O., Matthiopoulos, J., 2008. State-space models of individual animal movement. *Trends in Ecology & Evolution* 23, 87–94.
- Pewsey, A., Neuhäuser, M., Ruxton, G.D., 2013. *Circular Statistics in R*. Oxford University Press, Croydon.

- Plummer, M., Best, N., Cowles, K., Vines, K., 2006. Coda: Convergence diagnosis and output analysis for mcmc. *R News* 6, 7–11.
- Robert, C.P., Casella, G., 2005. Monte Carlo Statistical Methods (Springer Texts in Statistics). Springer-Verlag New York, Inc., Secaucus, NJ, USA.
- Sahu, S.K., Dey, D.K., Branco, M.D., 2003. A new class of multivariate skew distributions with applications to Bayesian regression models. *Canadian Journal of Statistics* 31, 129–150.
- Storch, K.F., Lipan, O., Leykin, I., Viswanathan, N., Davis, F.C., Wong, W.H., Weitz, C.J., 2002. Extensive and divergent circadian gene expression in liver and heart. *Nature* 417, 78–83.
- Wang, F., Gelfand, A., Jona Lasinio, G., 2015. Joint spatio-temporal analysis of a linear and a directional variable: space-time modeling of wave heights and wave directions in the Adriatic sea. *Statistica Sinica* 25, 25–39. doi:10.5705/ss.2013.204w.
- Wang, F., Gelfand, A.E., 2013. Directional data analysis under the general projected normal distribution. *Statistical Methodology* 10, 113–127.
- Wang, F., Gelfand, A.E., 2014. Modeling space and space-time directional data using projected Gaussian processes. *Journal of the American Statistical Association* 109, 1565–1580. doi:10.1080/01621459.2014.934454.

Appendix

A The invariance property of the \mathcal{PN}

Here we prove that the univariate marginal density of the circular variables is invariant. Let $\Theta_i^* = \delta(\Theta_i + \xi)$, where $\delta \in \{-1, 1\}$ and $\xi \in [0, 2\pi)$, following Theorem 1 of Mastrantonio et al. (2017), the density of $\Theta_i \sim \mathcal{PN}_1(\boldsymbol{\mu}_{w_i}, \boldsymbol{\Sigma}_{w_i})$, i.e., $f_{\Theta_i}(\cdot)$, has the invariant property if $f_{\Theta_i^*}(\cdot)$, i.e., the density of Θ_i^* , belongs to the same parametric family of $f_{\Theta_i}(\cdot)$.

The random variables Θ_i^* can be written as

$$\Theta_i^* = \text{atan}^* \frac{\sin \Theta_i^*}{\cos \Theta_i^*} = \text{atan}^* \frac{\sin(\delta(\Theta_i + \xi))}{\cos(\delta(\Theta_i + \xi))} = \text{atan}^* \frac{\delta \sin(\Theta_i + \xi)}{\cos(\Theta_i + \xi)}, \quad (\text{A.15})$$

and using relations $\cos(\alpha + \beta) = \cos \alpha \cos \beta - \sin \alpha \sin \beta$ and $\sin(\alpha + \beta) = \sin \alpha \cos \beta + \cos \alpha \sin \beta$, equation (A.15) can be stated equivalently as

$$\Theta_i^* = \text{atan}^* \frac{\delta(R_i \sin \Theta_i \cos \xi + R_i \cos \Theta_i \sin \xi)}{R_i \cos \Theta_i \cos \xi - R_i \sin \Theta_i \sin \xi} = \text{atan}^* \frac{\delta(W_{i2} \cos \xi + W_{i1} \sin \xi)}{W_{i1} \cos \xi - W_{i2} \sin \xi}.$$

To prove that Θ_i^* is \mathcal{PN} distributed, let consider the random variable $\mathbf{W}_i^* = \Delta \mathbf{T} \mathbf{W}_i$, where $\Delta = \text{diag}((1, \delta)^\top)$ and

$$\mathbf{T} = \begin{pmatrix} \cos \xi & -\sin \xi \\ \sin \xi & \cos \xi \end{pmatrix}.$$

\mathbf{W}_i^* is normally distributed and equation (1) applied to \mathbf{W}_i^* gives

$$\text{atan}^* \frac{W_{i2}^*}{W_{i1}^*} = \text{atan}^* \frac{\delta(W_{i2} \cos \xi + W_{i1} \sin \xi)}{W_{i1} \cos \xi - W_{i2} \sin \xi} = \Theta_i^*.$$

Then Θ_i^* follows a projected normal distribution; this proves the invariance of the \mathcal{PN} .

B MCMC implementation details

Sampling μ and Σ The full conditional of $\{\mu, \Sigma\}$ is proportional to

$$\prod_{t=1}^T \phi_{2p+q}((\mathbf{w}_t, \mathbf{y}_t)^\top - (\mathbf{0}_{2p}, \text{diag}(\boldsymbol{\lambda})\mathbf{d}_t)^\top | \mu, \Sigma) f(\mu, \Sigma | \boldsymbol{\lambda}). \quad (\text{B.16})$$

Equation (B.16) is equivalent to the full conditional of the mean and covariance matrix in a model with i.i.d. normally distributed observations. If we assume $f(\mu, \Sigma | \boldsymbol{\lambda}) \equiv f(\mu, \Sigma)$, with

$$f(\mu, \Sigma) \propto |\Sigma|^{-(\nu_0 + 2p + q)/2 - 1} \exp \left(-\frac{\text{tr}(\Psi_0 \Sigma^{-1}) + \kappa_0 (\mu - \mu_0)^\top \Sigma^{-1} (\mu - \mu_0)}{2} \right)$$

i.e., $f(\mu, \Sigma)$ is the density of a $\mathcal{NIW}(\mu_0, \kappa_0, \nu_0, \Psi_0)$, where $\kappa_0 > 0$ and $\nu_0 > 2p + q - 1$ are real numbers, $\mu_0 \in \mathbb{R}^{2p+q}$ and Ψ_0 is a $(2p + q) \times (2p + q)$ nnd matrix, and we let $\eta_t = (\mathbf{w}_t, \mathbf{y}_t)^\top - (\mathbf{0}_{2p}, \text{diag}(\boldsymbol{\lambda})\mathbf{d}_t)^\top$ and

$$\bar{\eta} = \frac{1}{T} \sum_{t=1}^T \eta_t,$$

the full conditional is $\mathcal{NIW}(\mu_{\text{post}}, \kappa_{\text{post}}, \nu_{\text{post}}, \Psi_{\text{post}})$ with

$$\begin{aligned} \mu_{\text{post}} &= \frac{\kappa_0 \mu_0 + T \bar{\eta}}{\kappa_0 + T}, \\ \kappa_{\text{post}} &= \kappa_0 + T, \\ \nu_{\text{post}} &= \nu_0 + T, \\ \Psi_{\text{post}} &= \Psi_0 + \sum_{t=1}^T (\eta_t - \bar{\eta})(\eta_t - \bar{\eta})^\top + \frac{\kappa_0 T}{\kappa_0 + T} (\bar{\eta} - \mu_0)(\bar{\eta} - \mu_0)^\top. \end{aligned}$$

Sampling λ The full conditional of λ is proportional to

$$\prod_{t=1}^T \phi_q(\mathbf{y}_t | \mu_{y_t|w_t} + \text{diag}(\mathbf{d}_t)\boldsymbol{\lambda}, \Sigma_{y|w}) g_2(\boldsymbol{\lambda}), \quad (\text{B.17})$$

where $\mu_{y_t|w_t} = \mu_y + \Sigma_{wy}^\top \Sigma_w^{-1} (\mathbf{w}_t - \mu_w)$ and $\Sigma_{y|w} = \Sigma_y - \Sigma_{wy}^\top \Sigma_w^{-1} \Sigma_{wy}$. In (B.17) we can see $\boldsymbol{\lambda}$ as a vector of regression coefficients, where the matrix of covariates is $\text{diag}(\mathbf{d}_t)$. Then, standard results tell us that a normal $g_2(\boldsymbol{\lambda})$ induces a normal full conditional. More precisely, let $\boldsymbol{\lambda} \sim \mathcal{N}_q(\gamma_0, \Omega_0)$, then the full conditional is $\mathcal{N}_q(\gamma_{\text{post}}, \Omega_{\text{post}})$ with

$$\begin{aligned} \Omega_{\text{post}} &= \left(\sum_{t=1}^T \text{diag}(\mathbf{d}_t) \Sigma_{y|w}^{-1} \text{diag}(\mathbf{d}_t) + \Omega_0^{-1} \right)^{-1}, \\ \gamma_{\text{post}} &= \Omega_{\text{post}} \left(\sum_{t=1}^T \text{diag}(\mathbf{d}_t) \Sigma_{y|w}^{-1} (\mathbf{y}_t - \mu_{y_t|w_t}) + \Omega_0^{-1} \gamma_0 \right). \end{aligned}$$

Sampling \mathbf{D}_t The full conditional of the latent vector \mathbf{D}_t is proportional to

$$\phi_q(\mathbf{y}_t | \mu_{y_t|w_t} + \text{diag}(\boldsymbol{\lambda})\mathbf{d}_t, \Sigma_{y|w}) \phi_q(\mathbf{d}_t | \mathbf{0}_q, \mathbf{I}_q).$$

\mathbf{d}_t can be seen as a vector of (positive) regressors with $\text{diag}(\boldsymbol{\lambda})$ as matrix of covariates and $\phi_q(\mathbf{d}_t|\mathbf{0}_q, \mathbf{I}_q)$ as prior. The full conditional is then $N_q(\mathbf{M}_{d_t}, \mathbf{V}_q) I_{\mathbf{0}_q, \infty}$, where $N_q(\cdot, \cdot) I_{\mathbf{0}_q, \infty}$ is a q -dimensional truncated normal distribution with components having support \mathbb{R}^+ ,

$$\mathbf{V}_d = \left(\boldsymbol{\Lambda}^\top \boldsymbol{\Sigma}_{y|w}^{-1} \boldsymbol{\Lambda} + \mathbf{I}_q \right)^{-1}$$

and

$$\mathbf{M}_{d_t} = \mathbf{V}_d \boldsymbol{\Lambda}^\top \boldsymbol{\Sigma}_{y|w}^{-1} \left(\mathbf{y}_t - \boldsymbol{\mu}_{y_t|w_t} \right).$$

Sampling R_{ti} Let $\mathbf{u}_{ti} = (\cos \theta_{ti}, \sin \theta_{ti})^\top$, $A_{ti} = \mathbf{u}_{ti}^\top \boldsymbol{\Sigma}_{w_{ti}|w_{t-i}, y}^{-1} \mathbf{u}_{ti}$ and $B_{ti} = \mathbf{u}_{ti}^\top \boldsymbol{\Sigma}_{w_{ti}|w_{t-i}, y}^{-1} \boldsymbol{\mu}_{w_{ti}|w_{t-i}, y_t}$, where $\boldsymbol{\mu}_{w_{ti}|w_{t-i}, y_t}$ and $\boldsymbol{\Sigma}_{w_{ti}|w_{t-i}, y}$ are the conditional mean and covariance matrix of \mathbf{w}_{ti} assuming $(\mathbf{w}_t, \mathbf{y}_t)^\top \sim \mathcal{N}_{2p+q}(\boldsymbol{\mu} + (\mathbf{0}_{2p}, \text{diag}(\boldsymbol{\lambda})\mathbf{d}_t)^\top, \boldsymbol{\Sigma})$. The full conditional of R_{ti} is then proportional to

$$r_{ti} \exp \left(-\frac{1}{2} A_{ti} \left(r_{ti} - \frac{B_{ti}}{A_{ti}} \right)^2 \right). \quad (\text{B.18})$$

Equation (B.18) is the same full conditional of the latent variable of the spherical \mathcal{PN} of Hernandez-Stumpfhauser et al. (2016) and then we can use their *slice sampling* strategy to sample from it.

In details, if

$$\begin{aligned} v_{ti} &\sim \mathcal{U} \left(0, \exp \left(-\frac{1}{2} A_{ti} \left(r_{ti} - \frac{B_{ti}}{A_{ti}} \right)^2 \right) \right), \\ v_{ti}^* &\sim \mathcal{U}(0, 1), \end{aligned}$$

then

$$r_{ti} = \sqrt{(\varrho_{2ti}^2 - \varrho_{1ti}^2) v_{ti}^* + \varrho_{1ti}^2},$$

with

$$\begin{aligned} \varrho_{1ti} &= \frac{B_{ti}}{A_{ti}} + \max \left\{ -\frac{B_{ti}}{A_{ti}}, -\sqrt{\frac{-2 \ln v_{ti}}{A_{ti}}} \right\}, \\ \varrho_{2ti} &= \frac{B_{ti}}{A_{ti}} + \sqrt{\frac{-2 \ln v_{ti}}{A_{ti}}}, \end{aligned}$$

is distributed accordingly to the full conditional (B.18).